NASA CONTRACTOR REPORT

APPLICATION OF APPROACH SPEED CRITERIA DERIVED FROM CLOSED-LOOP PILOT-VEHICLE SYSTEMS ANALYSES TO AN OGEE WING AIRCRAFT

by Richard J. Wasicko

Prepared by
SYSTEMS TECHNOLOGY, INC.
Hawthorne, Calif.
for Ames Research Center

NATIONAL AERONAUTICS AND SPACE ADMINISTRATION • WASHINGTON, D. C. • SEPTEMBER 1966

APPLICATION OF APPROACH SPEED CRITERIA DERIVED FROM CLOSED-LOOP PILOT-VEHICLE SYSTEMS ANALYSES TO AN OGEE WING AIRCRAFT

By Richard J. Wasicko

Prepared under Contract No. NAS 2-1868 by
SYSTEMS TECHNOLOGY, INC.
Hawthorne, Calif.

for Ames Research Center

NATIONAL AERONAUTICS AND SPACE ADMINISTRATION

For sale by the Clearinghouse for Federal Scientific and Technical Information
Springfield, Virginia 22151 – Price $2.50

FOREWORD

This report was prepared by Systems Technology, Inc., Hawthorne, California, under Task No. 1 of Contract No. NAS2-1868, "Master Agreement for Control Systems Analyses," with the National Aeronautics and Space Administration. The work was performed under the direction of the Flight and Systems Simulation Branch, Ames Research Center, with Mr. Maurice D. White serving as the NASA project monitor. The STI project technical director was Mr. Irving L. Ashkenas.

Mr. White and Mr. L. Stewart Rolls of the NASA assisted in obtaining airplane data and discussing the flight test program. Mr. Fred J. Drinkwater, III, supplied useful comments on piloting techniques in landing approaches and evaluation procedures to be used in the Ogee Wing F5D-1 tests. Mr. White reviewed the draft report and suggested several improvements. The careful work of the STI production staff in the preparation of this report is gratefully acknowledged.

ABSTRACT

Minimum comfortable approach speed criteria for aircraft carrier and airfield VFR landings are established from closed-loop pilot–vehicle analyses. The results are applied to an F5D-1 airplane modified with an ogee shaped wing. Drag characteristics and static longitudinal stability are varied and their effects on the predicted approach speeds are determined. The analysis indicates that for most of the configurations the approach speeds should not differ greatly for the two types of approaches, with the largest difference occurring for a low drag, high static margin configuration. A reduction in zero-lift drag or an increase in static longitudinal stability has an adverse effect on the predicted approach speeds.

CONTENTS

TABLES

FIGURES

SYMBOLS

A	Coefficient of term in reversal parameter numerator, Eq 10
$A_{q_i q_j}$	Coefficient of highest order s term in $N^{q_i q_j}_{\delta_e \delta_T}$
$A_{q_{i\delta}}$	Coefficient of highest order s term in $N_{q_{i\delta}}$
B	Coefficient of term in reversal parameter numerator, Eq 10
C	Coefficient of term in reversal parameter numerator, Eq 10
C_D	Drag coefficient
C_{D_u}	Nondimensional variation of drag coefficient with speed, $U_o \partial C_D / 2 \partial u$
C_{D_α}	Drag coefficient variation with angle of attack, $\partial C_D / \partial \alpha$, per rad
$C_{D_{\delta_e}}$	Drag coefficient variation with elevator deflection, $\partial C_D / \partial \delta_e$, per rad
C_L	Lift coefficient
C_{L_u}	Nondimensional variation of lift coefficient with speed, $U_o \partial C_L / 2 \partial u$
C_{L_α}	Lift coefficient variation with angle of attack, $\partial C_L / \partial \alpha$, per rad
$C_{L_{\delta_e}}$	Lift coefficient variation with elevator deflection, $\partial C_L / \partial \delta_e$, per rad
C_{m_q}	Pitch damping derivative, $\partial C_m / \partial (qc/2U_o)$
C_{m_α}	Pitching moment coefficient variation with angle of attack, $\partial C_m / \partial \alpha$, per rad
$C_{m_{\delta_e}}$	Pitching moment coefficient variation with elevator deflection, $\partial C_m / \partial \delta_e$, per rad
c	Mean aerodynamic chord, ft
$\bar{c}_{F5D}$	Mean aerodynamic chord of the basic F5D-1 airplane
D	Coefficient of term in reversal parameter numerator, Eq 10
D	Drag, lb
g	Acceleration due to gravity, 32.2 ft/sec^2
h	Displacement of the airplane normal to the steady-state flight path, positive upward, ft

I_{yy}	Moment of inertia about the Y axis, slug-ft^2
K_θ	Modified pilot describing function gain, $K_{\delta_e\theta}M_{\delta_e}/-M_\alpha$
$K_{\delta q_i}$	Frequency-invariant portion of the pilot describing function in the $q_i \rightarrow \delta$ loop
k_y	Radius of gyration about the Y axis, ft
L	Lift, lb
l_δ	Distance from airplane c.g. to elevator center of pressure, positive forward, ft
M_i	Rate of change of pitching acceleration (about the Y axis) due to perturbed motion quantity or control deflection
m	Mass, slugs
N	Numerator of reversal parameter, Eq 10
$N_{q_{i_\delta}}$	Numerator of q_i/δ_e or q_i/δ_T transfer function, particularized by substituting motion quantity involved for q_i
$N^{q_i q_j}_{\delta_e \delta_T}$	Coupling numerator, particularized by substituting motion quantities involved for q_i, q_j (see Appendix A)
q	Pitching velocity about the Y axis, rad/sec; general symbol for motion quantity
S	Reference wing area, ft^2
s	Laplace operator, $\sigma + j\omega$
T	Time constant, particularized by subscript, sec; airframe transfer function time constants shown in Table A-II
T	Thrust, lb
T_2	Time to double amplitude of speed instability, sec (Eq 19)
T_{δ_T}	Rate of change of thrust with throttle deflection, lb/rad
T_r	Thrust required for steady-state flight, lb
U_o	Linear steady-state velocity along the X stability axis, ft/sec, unless otherwise noted
u	Linear perturbed velocity along the X stability axis, ft/sec
V	Steady-state flight speed, kt

W	Weight, lb
w	Linear perturbed velocity along the Z axis, ft/sec
X_i	Rate of change of horizontal acceleration (along the X stability axis) due to perturbed motion quantity or control deflection
$Y_{\delta_e h}$	Pilot describing function in the h → δ_e loop
$Y_{\delta_e \theta}$	Pilot describing function in the θ → δ_e loop
Z_i	Rate of change of vertical acceleration (along the Z stability axis) due to perturbed motion quantity or control deflection
α	Perturbed angle of attack, rad or deg
α_T	Angle of attack of the thrust line, rad
γ	Flight path angle, positive upward, rad or deg
Δ	Increment change
Δ	Denominator of airframe transfer functions; characteristic equation when set equal to zero
δ_e	Elevator deflection, positive trailing edge down, rad or deg
δ_T	Throttle deflection, positive forward, rad
ζ_i	Damping ratio of linear second-order mode, particularized by subscript
θ	Perturbed pitch angle, positive upward, rad
ρ	Mass density of air, slugs/ft^3
σ	The real portion of the complex variable, $s = \sigma + j\omega$
τ	Time constant of speed instability, sec (Eq 19)
φ_m	Phase margin, deg
ω	Frequency, rad/sec; $j\omega$ is the imaginary portion of the complex variable, $s = \sigma + j\omega$
ω	Undamped natural frequency of a second-order mode, particularized by subscript, rad/sec
ω_c	Crossover frequency, frequency at which open-loop transfer function magnitude is unity, rad/sec

Subscripts:

db	Dive brakes
ϵ	Error
g	Landing gear
o	Conditions at $\zeta_p'' = 0$, as in ω_{p_o}'', and steady-state values, as in γ_o
p	Phugoid
sp	Short period

Special notes:

Primes on a transfer function or time constant indicate that it has been modified by inner loop closures, the number of primes corresponding to the number of closures.

The notation $\theta \rightarrow \delta_e$, $h \rightarrow \delta_T$ signifies that the pilot is controlling the aircraft's pitch attitude with elevator deflections and correcting altitude errors with the throttle. Other piloting techniques are represented by similar feedback-oriented symbols.

SECTION I

INTRODUCTION

Aircraft handling qualities in the approach and landing flight phase and criteria for predicting pilot-selected minimum comfortable approach speeds have been of considerable interest for many years. Research has concentrated on the problems of carrier and jet transport aircraft, and has attempted to determine the underlying factors involved in limiting approach speeds. In most of the work, flight test and simulation techniques have been used.

Prior to the introduction of high performance jet aircraft into military service in the post-World-War-II period, the method of estimating the approach speed as a fixed percentage of the power-approach configuration (gear and flaps down with power for level flight) stall speed was generally adequate for establishing carrier aircraft structural and arresting gear strength limits. The increased landing speeds of the sweptwing carrier aircraft with higher wing loadings which became operational in the early 1950's were of considerable concern, and an extensive program was undertaken by the NACA to investigate approach problems. Reference 1 summarizes in detail a major portion of the flight test results and reports the evaluation of various minimum approach speed criteria. Additional information, including test pilots' impressions of the piloting techniques used during carrier and airfield approaches, is contained in Refs. 2 and 3.

In recent years, the NASA has been investigating approach handling qualities of current subsonic and proposed supersonic jet transport configurations. Most of the effort has involved ground-based piloted simulator studies with emphasis on ILS approaches, although the last portion of the approach and the flare landing maneuver are simulated for minimum weather visual conditions (Ref. 4). As part of the general investigation of supersonic transport configurations and due to the

continued interest in approach problems, a program is under way at the NASA's Ames Research Center to flight test an F5D-1 aircraft modified with an ogee-shaped wing planform similar to that of a supersonic transport under development. The flight tests will establish minimum comfortable approach speeds for several types of landings, including a simulated mirror-aided carrier approach and a VFR approach with no flight path guidance, and will determine any unique low speed handling qualities of this configuration.

Most of the minimum approach speed criteria evaluated in Ref. 1 involved either a fixed percentage of some stall speed (determined from the maximum aerodynamic lift coefficient alone, the aerodynamic lift and a first-order estimate of the thrust contribution, or flight tests) or the minimum speed at which discrete maneuvers could be performed. None, however, evolved from considerations of the dynamic problems of the closed-loop pilot–vehicle system. Pilots reported that the primary factor influencing the minimum approach speed selection was "the ability to control altitude or arrest rate of sink," and this statement is sufficiently ambiguous to imply that the problem was difficult to localize in simple response terms and probably involved closed-loop pilot-vehicle interactions. Theorectical techniques for analyzing the pilot-vehicle combination and determining potential control difficulties have been developed and refined in recent years (Ref. 5 summarizes much of the work) and used to study longitudinal approach and landing problems of carrier aircraft (Refs. 5-7) and jet transports. The application of these techniques to low speed handling qualities considerations of the Ogee Wing F5D-1 airplane was the purpose of the study reported herein. The objectives have been to:

1. Obtain a better understanding of the handling qualities factors dictating pilot-selected minimum comfortable approach speeds and develop, where needed, criteria for different types of approaches.
2. Apply systems-analysis-derived criteria to predict Ogee Wing F5D-1 approach speeds in mirror-aided carrier approaches and VFR approaches for subsequent evaluation by flight tests.
3. Define considerations for the flight test program which might shed additional light on the basic factors of importance in approaches.

Factors other than closed-loop longitudinal control difficulties can influence a pilot's selection of a minimum approach speed; these were considered and found not to be limiting for the subject aircraft. For example, thrust margin available for go-around capability (Ref. 3) and over-the-nose visibility were not found critical for the Ogee Wing F5D-1 at speeds well below those considered limiting from closed-loop-derived criteria. Tail hook clearance at touchdown appeared to be a possible limiting factor, but discussions with a NASA test pilot during the course of the study revealed that the F5D-1 is basically a "four-wheeler," with initial touchdown contact on the aft wheel occurring quite often and not being regarded as a limiting factor. Lateral-directional handling qualities parameters showed, on the whole, a gradual deterioration with decreasing approach speeds, although several of these parameters, including the Dutch roll damping ratio, in fact actually improved at lower speeds. It was recognized that a progressive deterioration in the lateral-directional handling qualities might eventually result in an unsatisfactory pilot rating, with the gradual nature of the changes making it difficult to define a minimum comfortable approach speed. However, the generally adequate level of the lateral-directional parameters led to the conclusion that lateral-directional problems would not be critical or limiting for the Ogee Wing F5D-1.*

In view of these preliminary assessments and findings, the major emphasis of the remainder of the study was directed to longitudinal closed-loop control. The investigation presented in this report was performed prior to and during the initial phases of the flight test program. Certain aspects of the aircraft's approach configuration, including the center of gravity location and the gross weight, were not firmly established, and consequently preliminary estimates were

---

*The soundness of this decision was confirmed by recent NASA flight tests of the basic F5D-1 (Ref. 8), the results of which were published after this conclusion was reached. In these tests the lateral-directional stability and control characteristics were found to be acceptable for angles of attack up to 25 deg, which is well above the operating range of the Ogee Wing F5D-1 at approach speeds.

used in the computations. The validity of the approach speed criteria, as applied to the Ogee Wing F5D-1, must await the final pilot-selected minimum comfortable approach speeds determined from flight tests, and corrections to the predicted speeds should be made if the aircraft's flight configuration differs appreciably from that assumed in the analysis.

SECTION II

THE OGEE WING F5D-1 AIRPLANE

The Douglas F5D-1, a single-place high-performance fighter interceptor developed from the F4D-1, is a tailless configuration with a modified delta wing. The ogee wing version has leading edge extensions to achieve the desired planform and inlet ducts relocated approximately five feet forward. Side and plan view drawings of the F5D-1 and the ogee wing modification are shown in Fig. 1, and the main geometric differences are presented below. Reference 8 contains a detailed list of the physical characteristics of the basic F5D-1 configuration.

	Basic F5D-1	Ogee Wing F5D-1
Wing area, ft^2	557	661
Aspect ratio	2.02	1.70
Leading edge sweep at fuselage or duct, deg	52.5	77
Minimum leading edge sweep, deg.	52.5	55.8
Mean aerodynamic chord, ft	18.25	22.59
Location of quarter chord, F5D-1 fuselage station, inches	287.5	246.5

Longitudinal force and moment coefficient characteristics for the approach configuration, obtained from full scale power-off tests in the 40-ft by 80-ft wind tunnel at the Ames Research Center, are shown in Fig. 2. In these tests the trimmer or inboard elevon was not deflected, the dive brakes were closed, and the landing gear was down. The moment reference is at 15 percent of the basic F5D-1 mean aerodynamic chord ($0.15\ \bar{c}_{F5D}$). Throughout this report, center of gravity locations are specified in terms of $\bar{c}_{F5D}$.

There is no stall break in the lift coefficient data in the angle of attack range up to 21 deg, and with the c.g. at $0.15\ \bar{c}_{F5D}$ the static margin is less than 5 percent for trimmed lift coefficients from 0.4

to 0.7. The lowest static margin occurs at a trimmed lift coefficient of approximately 0.5 and is slightly greater than 1 percent. Additional power-on tests at thrust coefficients of 0.116 and 0.184 indicated no pitching moment due to thrust.

The initial flight test plans called for a landing configuration with the gear down, dive brakes closed, trimmer undeflected, a gross weight of 19,700 lb, and the center of gravity at about 0.148 to 0.15 $\bar{c}_{F5D}$. The latter was selected as a nominal location for subsequent analyses. Stability and control derivatives and transfer function characteristics for this configuration are presented in Appendix A.

The aerodynamic characteristics of the Ogee Wing F5D-1 in the approach flight phase can be altered to some degree by changing the zero-lift drag. This is accomplished by extending or retracting the landing gear and dive brakes. Based on wind tunnel results, the dive brakes produce an incremental drag coefficient of $\Delta C_{D_{db}} = 0.0188$, a small nose-up zero-lift pitching moment, and no change in the lift coefficient and pitching moment coefficient variations with angle of attack up to 13 deg. At higher angles of attack with the dive brakes deployed there is a reduction in both the lift curve slope and the static longitudinal stability. A landing gear drag coefficient increment of $\Delta C_{D_g} = 0.015$ was obtained from Ref. 9. These values, which were used in the subsequent analyses, were substantiated by preliminary flight test data for the Ogee Wing F5D-1 which indicated $\Delta C_{D_{db}} \doteq 0.02$ and $\Delta C_{D_g} \doteq 0.015$.

SECTION III

MINIMUM APPROACH SPEEDS FOR CARRIER LANDINGS

A criterion for predicting minimum acceptable carrier approach speeds was developed in Refs. 5 and 6 from a closed-loop pilot-vehicle systems analysis. Assuming the pilot controlled pitch attitude with the elevator ($\theta \rightarrow \delta_e$) and corrected altitude errors, or deviations from the desired flight path, with throttle application ($h \rightarrow \delta_T$), it was found that a deterioration in altitude tracking performance with increased tightness of the pitch attitude loop could occur when the approach speed was reduced below a certain value. The simple analytical expression for this effect was termed the "reversal parameter," and the criterion speed was that at which the parameter changed to a negative sign. Flight test minimum approach speeds for five out of seven aircraft limited by "ability to control altitude or arrest rate of sink" were found to agree closely with the speeds predicted theoretically (Ref. 6), and a fixed-base simulator study (Ref. 7) performed to test the theory generally supported its validity.

Reference 6 indicates that the piloting technique assumed in the derivation of the reversal parameter does not achieve the best tracking performance, and offers several possible explanations for the pilot's selection of nonoptimum control feedbacks. In a more recent study of carrier landings (Ref. 10), the terminal dispersions due to ship motions and atmospheric turbulence were determined for two aircraft control methods, the first involving altitude control with throttle and pitch attitude control with elevator ($h \rightarrow \delta_T$, $\theta \rightarrow \delta_e$) and the second using altitude and pitch attitude control with elevator and airspeed control with throttle ($h,\theta \rightarrow \delta_e$, $u \rightarrow \delta_T$). The former resulted in excessively large ramp clearance and touchdown dispersions, and it was concluded that the latter piloting technique must be used when approaching the ramp. (The airspeed-to-throttle loop stabilizes the slow divergence due to $h \rightarrow \delta_e$ control when operating on the back side of the drag curve and would be essential if this technique were used throughout the complete approach. It is not needed during the last few seconds of a carrier

approach because the divergence, primarily in airspeed, cannot build up to a critical level in the short time periods involved.) The slower responding and simpler (two loop closures as opposed to three) $h \rightarrow \delta_T$, $\theta \rightarrow \delta_e$ method is adequate in the initial approach phases (approach to and acquisition of the glide slope beam) where precise altitude error information is not available and tight control is not required. Thus, although the same piloting technique is not used during all portions of the approach, the minimum approach speed should be predictable from an analysis of the phase which is most speed-critical. The approach is, or should be, made at a constant speed, and if a reversal effect can occur during the early phase, this consideration can dictate the minimum speed selected for the complete approach.

The applicability of the reversal parameter criterion for predicting approach speeds of the low static margin Ogee Wing F5D-1 was somewhat uncertain, initially, because of the following factors:

1. In the original derivation of the reversal parameter, only the phugoid motions were considered. Assuming the factors which limited the approach speed were primarily associated with the low-frequency behavior of the pilot-vehicle system, neglect of the higher frequency short-period effects seemed reasonable and also permitted the development of an approach speed criterion in analytical form. For configurations having a low static margin, the reduced short-period frequency might couple or interact with the phugoid mode and possibly invalidate the simplified analysis.

2. Theoretically, for identically zero static margin ($M_\alpha = 0$) and no thrust offset, there is no reversal effect, and the influences of control actions are completely separated (Ref. 7). The $\theta \rightarrow \delta_e$ loop does not modify the phugoid characteristics and hence does not interact with the outer loop throttle control of altitude errors.

3. A limited series of experiments (Ref. 7) indicated that with zero thrust offset a marked reduction in the effects of airframe configuration characteristics on pilot rating occurred when $-M_\alpha$ was reduced from 6.07 to 0.903.

These uncertainties are removed by the detailed considerations which follow. The basic influence of static longitudinal stability on the reversal parameter is developed, and carrier approach speed predictions are made for several drag configurations of the Ogee Wing F5D-1 with different c.g. locations.

A. EVALUATION OF THE REVERSAL PARAMETER FOR LOW STATIC MARGIN CONFIGURATIONS

The reversal phenomenon concerns the effect of the inner attitude loop gain on ω_p'', the final closed-loop phugoid frequency at which oscillations in altitude will occur. The bandwidth of the outer loop is related to ω_p'' and to ω_{p_o}'', the value of ω_p'' when the pilot's altitude-to-throttle gain is increased sufficiently to cause the final closed-loop phugoid damping ratio to be zero. The analytical expression describing the reversal phenomenon is based on the following assumptions:

1. The pilot controls pitch attitude with the elevator and altitude with the throttle, and his describing function can be approximated by a pure gain in both loops.

2. The vehicle's short-period dynamics can be neglected.

3. Throttle deflection does not produce a pitching moment.

4. The final closed-loop phugoid frequency at zero damping ratio, ω_{p_o}'', is a convenient and pertinent measure of performance.

The main concern is the validity of Assumption 2 for the low M_α conditions of interest in the case of the Ogee Wing F5D-1. This is resolved by comparing results using only the phugoid dynamics with those obtained when both the phugoid and short-period are considered. From the reversal parameter derivation (Ref. 6), the square of ω_{p_o}'' is given by

$$\left(\omega_{p_o}''\right)^2 = \frac{\frac{1}{T_{h_T}}\left(\omega_p^2 + K_\theta \frac{1}{T_{\theta_1} T_{\theta_2}}\right)}{\left[(1 + K_\theta)\frac{1}{T_{h_T}} - 2\zeta_p\omega_p - K_\theta\left(\frac{1}{T_{\theta_1}} + \frac{1}{T_{\theta_2}}\right)\right]} \qquad (1)$$

where $K_\theta = K_{\delta_e\theta} M_{\delta_e} / -M_\alpha$ and the other terms are vehicle transfer function parameters. $(\omega_{p_o}'')^2$ as expressed by Eq 1 can be plotted versus K_θ. Similarly, $(\omega_{p_o}'')^2$ can be found from multiloop $\theta \rightarrow \delta_e$, $h \rightarrow \delta_T$ closures using complete transfer function expressions. In this case, the outer open-loop transfer function describing the aircraft's altitude response, h,

to the pilot-observed altitude error, h_ϵ, with both the pitch attitude and altitude loops closed by pure-gain representations for the pilot ($K_{\delta_e\theta}$ and $K_{\delta_T h}$ respectively) is (Ref. 6)

$$\left(\frac{h}{h_\epsilon}\right)_{\substack{\theta\rightarrow\delta_e \\ h\rightarrow\delta_T}} = \frac{K_{\delta_T h}\left(N_{h_{\delta_T}} + K_{\delta_e\theta}N^{\theta\ h}_{\delta_e\delta_T}\right)}{\Delta + K_{\delta_e\theta}N_{\theta_{\delta_e}}} \tag{2}$$

where

$$\Delta = \left(s^2 + 2\zeta_p\omega_p s + \omega_p^2\right)\left(s^2 + 2\zeta_{sp}\omega_{sp}s + \omega_{sp}^2\right)$$

$$N_{\theta_{\delta_e}} = M_{\delta_e}\left(s + \frac{1}{T_{\theta_1}}\right)\left(s + \frac{1}{T_{\theta_2}}\right)$$

$$sN_{h_{\delta_T}} = -Z_{\delta_T}\left(s + \frac{1}{T_{h_T}}\right)\left(s^2 + 2\zeta_h\omega_h s + \omega_h^2\right)$$

$$sN^{\theta\ h}_{\delta_e\delta_T} = -Z_{\delta_T}M_{\delta_e}\left(s + \frac{1}{T_{\theta h}}\right)$$

(The gain in the $sN^{\theta\ h}_{\delta_e\delta_T}$ expression is that for $M_{\delta_T} = 0$ and is applicable for the Ogee Wing F5D-1.) When the inner θ loop is closed at a particular value of the pilot's gain $K_{\delta_e\theta}$, Eq 2 becomes

$$\left(\frac{h}{h_\epsilon}\right)_{\substack{\theta\rightarrow\delta_e \\ h\rightarrow\delta_T}} = \frac{-K_{\delta_T h}Z_{\delta_T}\left(s + \frac{1}{T'_{h_T}}\right)\left(s^2 + 2\zeta'_h\omega'_h s + \omega'^2_h\right)}{s\left(s^2 + 2\zeta'_p\omega'_p s + \omega'^2_p\right)\left(s^2 + 2\zeta'_{sp}\omega'_{sp}s + \omega'^2_{sp}\right)} \tag{3}$$

The frequency at which the Bode phase angle of Eq 3 equals −180 deg is ω''_{p_o}.

Results derived from the complete expressions involving both the phugoid and short-period modes and those obtained when only the phugoid is considered (using Eq 1) are compared in Fig. 3 for two flight conditions, one above and one below the reversal, or $\partial(\omega''_{p_o})^2/\partial K_\theta = 0$, speed.* The more complete solution yields values of ω''_{p_o} slightly less than those determined from Eq 1, but the variation with K_θ, which is the effect of

*The effects of varying M_α are included in both methods, since both use exact vehicle transfer function parameters.

interest, is similar in both cases and hence the reversal speeds are not significantly different. (For example, linear interpolation between the two speeds shown in Fig. 3 gives less than 1 kt variation in reversal speed for the two techniques when pertinent values of K_θ, from 1 to 3, are used.) Although with the nominal c.g. location at 0.15 $\bar{c}_{F5D}$ the static margins of the Ogee Wing F5D-1 are quite low, the maneuver margins are large enough so that short-period frequencies are separated from phugoid frequencies by about a factor of 10 (see Table A-II) and there is no appreciable interaction. Therefore the simplified analysis applies, provided that the reversal effect is indeed the applicable limiting phenomenon.

In this connection, the correlation of flight-test approach speeds with the simplified reversal parameter lends support to its use in the present case. Figure 4 shows the approach regime short-period characteristics of the seven aircraft used to test the reversal parameter criterion. As noted in Ref. 6, the flight-test minimum approach speeds agreed rather well with the speeds corresponding to $\partial(\omega''_{p_o})^2/\partial K_\theta = 0$ for the five aircraft which exhibited reversal. One of these, the F8U-1, has a low short-period frequency, about 1 rad/sec, approximately the same as that of the Ogee Wing F5D-1.

These optimistic conclusions regarding the applicability of the simple reversal criterion are not completely borne out by the results of the reduced-M_α experiments reported in Ref. 7. As shown in Fig. 5,* there is no correlation of pilot rating with the reversal parameter for the twelve zero thrust offset configurations tested, and the ratings in general are insensitive to changes in vehicle dynamics. Four configurations (C5, C7, C13, and C16) have quite large negative values of the reversal parameter. The median ratings vary between 2.0 and 3.5 and in all cases are better than the average results (shown by the solid line

*In Ref. 7 the data were presented as median pilot rating versus the reversal parameter associated with the original high-M_α transfer function characteristics. Reducing M_α, while normally having a small effect on the transfer function factors in the reversal parameter expression, can have a pronounced influence on the numerical value of the reversal parameter itself. The reversal parameter values in Fig. 5 were computed from transfer function factors which reflected M_α effects.

in Fig. 5) obtained for the high-M_α configurations.

Unfortunately, the low-M_α experiments of Ref. 7 were very limited, were performed after the high-M_α tests, and involved only a single evaluation of each configuration by each of three participating pilots. In the main experiment of Ref. 7 with high-M_α vehicle dynamics, these same pilots, when rating the questionable C5, C7, C13, and C16 configurations, delivered average ratings considerably higher than those indicated in Fig. 5. However, in the course of repeated tests, each of the pilots also delivered minimum ratings about equal to those shown for all twelve configurations. For the most part, these minimum ratings were given after considerable learning of the high-M_α task and just before the low-M_α runs. Therefore, the apparent favorable effect of reduced M_α implied by Fig. 5 may actually reflect an improvement in pilot rating due to experience and training with the simulated carrier landing task. Because of this fact, some uncertainty remains with respect to valid M_α effects on the reversal phenomenon.

B. STATIC MARGIN EFFECTS ON THE REVERSAL PARAMETER

The reversal phenomenon associated with $\theta \rightarrow \delta_e$, $h \rightarrow \delta_T$ control is a low-frequency effect involving the closed-loop phugoid motion of the pilot-airframe combination. As shown previously, the loop closure behavior is adequately described when only the phugoid mode of the vehicle transfer functions is used. However, the phugoid characteristics as well as the θ/δ_e numerator factors are influenced by variations in M_α, and such changes can combine to produce pronounced effects on the reversal parameter value and on the associated predicted approach speed.

The simple zero-thrust-offset reversal parameter expression is (Ref. 6)

$$\frac{\partial(\omega''_{p_o})^2}{\partial K_\theta} = \frac{\frac{1}{T_{\theta_1}T_{\theta_2}}\left(\frac{1}{T_{h_T}} - 2\zeta_p\omega_p\right) + \omega_p^2\left(\frac{1}{T_{\theta_1}} + \frac{1}{T_{\theta_2}} - \frac{1}{T_{h_T}}\right)}{T_{h_T}\left[\left(1 + K_\theta\right)\frac{1}{T_{h_T}} - 2\zeta_p\omega_p - K_\theta\left(\frac{1}{T_{\theta_1}} + \frac{1}{T_{\theta_2}}\right)\right]^2} \qquad (4)$$

The sign of the reversal parameter is determined by the sign of the Eq 4

numerator, which is composed of two terms of approximately equal magnitude, the first term normally positive and the second negative. Any configuration change which increases the magnitude of the first term and/or decreases the magnitude of the second term is favorable with regard to lowering the predicted approach speed. Exact and approximate relations for the various transfer function terms in Eq 4 as functions of dimensional stability and control derivatives (for the zero-thrust-offset, or $M_u = 0$, condition) are

$$\frac{1}{T_{\theta_1}} + \frac{1}{T_{\theta_2}} = -X_u - Z_w + \frac{M_\alpha}{U_o}\frac{Z_{\delta_e}}{M_{\delta_e}} \tag{5}$$

$$\frac{1}{T_{\theta_1}}\frac{1}{T_{\theta_2}} = X_u Z_w - Z_u X_w + \frac{M_\alpha}{U_o}\left(Z_u \frac{X_{\delta_e}}{M_{\delta_e}} - X_u \frac{Z_{\delta_e}}{M_{\delta_e}}\right) \tag{6}$$

$$\frac{1}{T_{h_T}} = -X_u + Z_u \frac{X_{\delta_T}}{Z_{\delta_T}} \tag{7}$$

$$\omega_p^2 \doteq -\frac{gZ_u}{U_o}\left(\frac{M_\alpha}{M_\alpha - Z_w M_q}\right) \tag{8}$$

$$2\zeta_p\omega_p \doteq -X_u \tag{9}$$

The effect of static margin is indicated by the influence of M_α in Eqs 5, 6, and 8 and the corresponding location of the transfer function terms in the reversal parameter numerator.* Decreasing the static margin causes the following to occur:

1. ω_p^2 decreases, reducing the magnitude of the second term in the reversal parameter numerator, and always producing a beneficial lowering of the predicted approach speed.

*This method of assessing reversal parameter numerator components also indicates other beneficial configuration changes. For example, Ref. 6 noted that the inclusion of X_{δ_e} was favorable for approach speed predictions of the F4D-1; without X_{δ_e} the reversal parameter was negative at all speeds tested (Fig. 4). X_{δ_e} occurs only in Eq 6, and since M_α, Z_u, X_{δ_e}, and M_{δ_e} are all negative, increasing the magnitude of X_{δ_e} increases $(1/T_{\theta_1})(1/T_{\theta_2})$ and consequently the first term in the reversal parameter numerator. However, it should be noted that the F4D-1 has an unusually high value of M_α in the approach speed region (indicated by the relatively large values of ω_{sp} in Fig. 4) and hence the favorable effect of elevator drag is more pronounced for this aircraft.

2. $\left|(1/T_{\theta_1}) + (1/T_{\theta_2})\right|$ increases in a favorable manner for aft elevator ($Z_{\delta_e}/M_{\delta_e} > 0$) aircraft.

3. $\left|(1/T_{\theta_1})(1/T_{\theta_2})\right|$ increases, and this lowers the predicted approach speed if $\left|Z_u(X_{\delta_e}/M_{\delta_e}) - X_u(Z_{\delta_e}/M_{\delta_e})\right|$ is positive. Using the identities $-Z_u = 2g/U_o$, $X_u/Z_u = C_D/C_L$ and $C_{m_{\delta_e}} = (l_\delta/c)C_{L_{\delta_e}}$ where l_δ is positive forward, this term can be written

$$Z_u \frac{X_{\delta_e}}{M_{\delta_e}} - X_u \frac{Z_{\delta_e}}{M_{\delta_e}} = \frac{2gk_y^2}{U_o l_\delta}\left[\frac{C_{D_{\delta_e}}}{C_{L_{\delta_e}}} - \frac{C_D}{C_L}\right]$$

and is positive when an aft elevator has a higher lift/drag ratio than the airplane itself.

For the Ogee Wing F5D-1, $C_{L_{\delta_e}}/C_{D_{\delta_e}} > C_L/C_D$ (see Table A-I) and reducing the static margin has a beneficial effect on all three terms.

It is not possible to generalize in a simple manner the effects of static longitudinal stability on the reversal parameter, particularly for a canard configuration with $C_{L_{\delta_e}}/C_{D_{\delta_e}} > C_L/C_D$ or an aft elevator aircraft with $C_{L_{\delta_e}}/C_{D_{\delta_e}} < C_L/C_D$. The numerator, N, of the reversal parameter can be written

$$N = A + BM_\alpha + C\frac{M_\alpha}{M_\alpha - Z_w M_q} + D\frac{M_\alpha^2}{M_\alpha - Z_w M_q} \qquad (10)$$

where

$$A = Z_u \frac{X_{\delta_T}}{Z_{\delta_T}}\left(X_u Z_w - Z_u X_w\right)$$

$$B = \frac{Z_u}{U_o}\frac{X_{\delta_T}}{Z_{\delta_T}}\left(Z_u \frac{X_{\delta_e}}{M_{\delta_e}} - X_u \frac{Z_{\delta_e}}{M_{\delta_e}}\right)$$

$$C = \frac{gZ_u}{U_o}\left(Z_w + Z_u \frac{X_{\delta_T}}{Z_{\delta_T}}\right)$$

$$D = -\frac{gZ_u}{U_o^2}\frac{Z_{\delta_e}}{M_{\delta_e}}$$

The partial derivative with respect to M_α is

$$\frac{\partial N}{\partial M_\alpha} = B + D - \frac{Z_w M_q \left(C + Z_w M_q D\right)}{\left(M_\alpha - Z_w M_q\right)^2} \tag{11}$$

and it can be seen that the rate of change of the reversal parameter numerator with M_α depends on M_α as well as the other stability and control derivatives. A positive value of $\partial N/\partial M_\alpha$ indicates a favorable effect of reducing the static longitudinal stability. If M_α is large and hence, from Eq 8, $\omega_p^2 \doteq -gZ_u/U_o$, Eq 11 becomes

$$\frac{\partial N}{\partial M_\alpha} \doteq B + D \tag{12}$$

which, using the previous identities and $X_{\delta_T}/Z_{\delta_T} = -1/\alpha_T$, can be expressed in nondimensional form as

$$\frac{\partial N}{\partial M_\alpha} \doteq -\frac{\rho g k_y^2 S C_D}{m U_o l_\delta}\left[\frac{2}{\alpha_T}\left(1 - \frac{C_L}{C_D}\frac{C_{D_{\delta_e}}}{C_{L_{\delta_e}}}\right) + \frac{C_L}{C_D}\right] \tag{13}$$

C. PREDICTED APPROACH SPEEDS FOR THE OGEE WING F5D-1

The previous considerations have shown that the simple reversal parameter (Eq 4) should be applicable to the low static margin Ogee Wing F5D-1 and that a significant M_α effect may exist. Carrier approach speed predictions are made for the basic configuration, with the landing gear down, dive brakes closed, and a gross weight of 19,700 lb, and for low and high drag configurations obtained by changing the gear and dive brake positions.* For the nominal c.g. location at 0.15 $\bar{c}_{F5D}$, the reversal

*It is assumed the landing gear and dive brakes change only the drag coefficient and hence only the X_u derivative is modified. The incremental drag coefficients are given in Section II.

parameter predicted approach speeds are:

CONFIGURATION	GEAR	DIVE BRAKES	U_o (knots)
Basic.....	Down	Closed	123
Low drag.....	Up	Closed	128
High drag.....	Down	Open	118

Static margin effects on the approach speed are shown in Fig. 6 for the three configurations. Revised trim characteristics were not determined for the different c.g. locations indicated, and except for M_α the dimensional stability and control derivatives for the nominal 0.15 $\bar{c}_{F5D}$ location were used in each case to calculate the reversal parameter.

A change in the zero-lift drag coefficient has an appreciable effect on the predicted approach speeds, with a 10 knot difference existing between the low and high drag configurations. M_α effects are also important, and Fig. 6 indicates that a five percent forward shift in the c.g. location (based on $\bar{c}_{F5D}$ and corresponding to 11 inches) for the basic configuration raises the predicted approach speed 5.5 knots. Approximately the same speed–c.g. sensitivity exists for the high drag configuration (Fig. 6c). However, the low drag configuration <u>may</u> have a quite large variation of approach speed with static margin, particularly for c.g.'s around 0.12 $\bar{c}_{F5D}$. The "exact" variation of predicted approach speed with c.g. in this case depends strongly on the fairings used in Fig. 6b <u>and</u> on the criterion value assigned to the reversal parameter. The criterion $\partial(\omega''_{p_o})^2/\partial K_\theta = 0$ was originally chosen (Ref. 6) because it was convenient and because finite values other than, but close to, zero made little difference in the associated speed. This is not true in the case of the low drag configuration with c.g. locations forward of the nominal 0.15 $\bar{c}_{F5D}$ position. Figure 6b shows that for the 0.12 $\bar{c}_{F5D}$ c.g. location a criterion change from zero to ±0.001 involves predicted approach speed changes of about ±8 knots. Flight tests of this particular

configuration with c.g.'s forward to the 0.10 $\bar{c}_{F5D}$ location might be especially revealing as to the validity of a specific value of $\partial(\omega''_{p_o})^2/\partial K_\theta$ as a criterion. On the other hand, the shallow slope of the reversal parameter versus approach speed curve might reflect itself as difficulty on the part of the pilot to define a specific minimum approach speed. This, however, would indicate the importance of the reversal phenomenon.

SECTION IV

APPROACH SPEEDS FOR VISUAL FLIGHT CONDITIONS

In VFR approaches the pilot does not have available to him precise information on aircraft vertical deviations from the desired flight path. The lack of a definite flight path error signal distinguishes the airfield VFR case from carrier landings and airfield IFR landings where the respective altitude errors are obtained from the optical landing aid and the glide slope indicator. The central questions involved in manual VFR approaches relate to what information is sensed by the pilot from the external field of view (and from cockpit instruments) and how such information is used to control the vehicle.

A. POSSIBLE PILOTING TECHNIQUES

As noted in Section III, the $\theta \rightarrow \delta_e$, $h \rightarrow \delta_T$ piloting technique used to derive the reversal parameter carrier approach speed criterion applies for the initial approach phases where precise altitude error information is not available and tight control is not required. To a certain extent, this situation corresponds to the VFR approach case, and the $\theta \rightarrow \delta_e$, $h \rightarrow \delta_T$ technique has the attractive feature of being stable on the initial portion of the back side of the drag curve, although it may experience a reversal phenomenon at lower speeds. If in fact it applies for VFR approaches, minimum acceptable speeds should be those predicted by a sign change, or reversal, of the parameter $\partial(\omega''_{p_o})^2/\partial K_\theta$. However, other considerations presented in the following development suggest a different criterion.

For airfield IFR landings there is strong evidence that pilots control attitude and altitude with the elevator ($\theta, h \rightarrow \delta_e$). This appears to be a more natural piloting technique, and on the front side of the drag curve can result in stable closed-loop characteristics with good tracking performance. On the back side of the drag curve, however, the

low frequency zero, $1/T_{h_1}$, in the numerator of the altitude-to-elevator transfer function is in the right half portion of the s-plane and the outer $h \rightarrow \delta_e$ closure produces an instability, occurring predominantly in airspeed. This speed divergence can be controlled with an additional $u \rightarrow \delta_T$ loop. For VFR landings, there is no direct experimental evidence that this piloting technique is used, although it offers good flight path control. The closure characteristics of this technique will be examined in more detail to determine any limiting behavior similar to the reversal phenomenon for the $\theta \rightarrow \delta_e$, $h \rightarrow \delta_T$ technique.

A representative example is shown in Fig. 7 for the Ogee Wing F5D-1 at the nominal c.g. of 0.15 $\bar{c}_{F5D}$ and an approach speed of 131 knots. The pilot describing function for the inner pitch attitude loop is $Y_{\delta_e\theta} = K_{\delta_e\theta} e^{-0.3s}$, with $K_{\delta_e\theta} = -0.33$ deg/deg, and for the outer altitude loop is a pure gain,* $K_{\delta_e h}$. The criterion for the final closure is somewhat arbitrary, and in this case was to set the damping ratio of the closed-loop phugoid mode at 0.35. The altitude tracking capability is good, with a high crossover frequency and high effective closed-loop bandwidth. The free s in the denominator of h/h_ϵ is driven near $1/T_{h_1}$ and the closed-loop instability represented by $1/T''_{h_1}$ is not dominant in the altitude response.

Table I summarizes the closed-loop dynamics, crossover frequencies, and phase margins obtained by constructions similar to Fig. 7 for a series of approach speeds; also shown is the pilot's elevator-to-altitude error gain required for $\zeta''_p = 0.35$. Most of the parameters do not vary appreciably with airspeed. However, there is a gradual reduction in bandwidth (revealed by the decreasing crossover frequency) and an increase in the magnitude of the inverse time constant of the unstable mode. The latter can be stabilized by the pilot with an airspeed-to-throttle loop which will not have a major influence on the other closed-loop modes. With the

*In the frequency region of interest, $\omega \doteq 0.5$ rad/sec, the phase lag due to a 0.3 sec pilot reaction time delay is only 9 deg and therefore is not of significance.

$\theta,h \rightarrow \delta_e$ loops closed, the $u \rightarrow \delta_T$ transfer function,

$$\left(\frac{u}{\delta_T}\right)_{\theta,h\rightarrow\delta_e} = \frac{N_{u\delta_T} + Y_{\delta_e\theta}N^{\theta\ u}_{\delta_e\delta_T} + Y_{\delta_eh}N^{h\ u}_{\delta_e\delta_T}}{\Delta + Y_{\delta_e\theta}N_{\theta\delta_e} + Y_{\delta_eh}N_{h\delta_e}} \tag{14}$$

for this series of approach speeds can be approximated by a single first-order term, i.e.,

$$\left(\frac{u}{\delta_T}\right)_{\theta,h\rightarrow\delta_e} \doteq \frac{X_{\delta_T}}{\left(s + \frac{1}{T''_{h_1}}\right)} \tag{15}$$

Pilot control of this slow divergence is easily achieved, and the pilot's throttle-to-airspeed gain required for neutral stability is $K_{\delta_T u} = -1/X_{\delta_T}T''_{h_1}$. Since X_{δ_T} does not vary with airspeed $\left[X_{\delta_T} \doteq (1/m)T_{\delta_T}\right]$, the necessary pilot gain and hence the amount of throttle activity is directly proportional to $1/T''_{h_1}$ and increases as the approach speed decreases. Since $1/T''_{h_1}$ is approximately proportional to $1/T_{h_1}$, the control difficulty is directly related to the low frequency zero in the airframe's altitude-to-elevator transfer function.

If the pilot were able to directly determine precise flight path (or altitude) error information in a VFR landing, the above considerations would be of direct interest. He may or may not be able to extract such information from the external field of view, and he may be more concerned with the terminal conditions at touchdown than with flight path errors. Rather than correct altitude errors, even when sensed, the pilot may instead merely alter the rate of sink, establishing a new flight path with the same terminal point on the runway. In this case, $\dot{h}$ rather than h is the appropriate outer loop feedback quantity. To achieve good $\dot{h}$ tracking performance, the pilot must generate a low frequency lag in the $\dot{h} \rightarrow \delta_e$ final closure. Consequently, the closed-loop dynamics achieved when a $\theta,\dot{h} \rightarrow \delta_e$ technique is used are similar to those obtained for the $\theta,h \rightarrow \delta_e$ closure. The only apparent significant effect of reduced approach speeds

is an increase in the magnitude of the unstable inverse time constant, $1/T''_{h_1}$, which again is approximately proportional to $1/T_{h_1}$.

Whether the pilot maintains tight flight path control with the elevator or simply adjusts the rate of sink with elevator, the deterioration in closed-loop characteristics is progressive with decreasing approach speeds. The most pronounced change is the required increase in throttle activity, which is approximately proportional to $1/T_{h_1}$. This result suggests the use of the open-loop parameter $1/T_{h_1}$ as a possible measure of piloting difficulty for VFR approaches. The limiting factor for the $\theta,h \rightarrow \delta_e$, $u \rightarrow \delta_T$ piloting technique, however, does not have the distinct behavior of the reversal phenomenon associated with $\theta \rightarrow \delta_e$, $h \rightarrow \delta_T$ control.

B. AVAILABLE EXPERIMENTAL DATA

The probable maximum negative value of $1/T_{h_1}$ acceptable to pilots in VFR approaches can be deduced from information contained in Refs. 11 – 13. Values of $1/T_{h_1}$ are not presented explicitly in these reports; however, the reports do contain aerodynamic and other characteristics required to compute them approximately. For $X_{\delta_e} = 0$, from Ref. 14,

$$\frac{1}{T_{h_1}} \doteq \frac{\rho S U_o}{m}\left[C_D + C_{D_u} - \frac{C_{D_\alpha}}{C_{L_\alpha}}\left(C_L + C_{L_u}\right)\right] \tag{16}$$

[An additional term, $-(1/m)(\partial T/\partial u)$, is added to Eq 16 when thrust variations with speed are significant (Ref. 7).] For C_{D_u} and C_{L_u} negligible and using the basic lift equation, $L = W = (1/2)\rho U_o^2 S C_L$,

$$\frac{1}{T_{h_1}} \doteq \frac{2g}{U_o}\left(\frac{C_D}{C_L} - \frac{C_{D_\alpha}}{C_{L_\alpha}}\right) = \frac{2g}{U_o}\left(\frac{C_D}{C_L} - \frac{dC_D}{dC_L}\right) \tag{17}$$

Also, from Ref. 7,

$$\frac{1}{T_{h_1}} \doteq \frac{1}{m}\left(\frac{dD}{du} - \frac{\partial T}{\partial u}\right) \tag{18}$$

where dD/du is the <u>total</u> variation of drag with airspeed for constant lift evaluated at the trimmed airspeed.

Reference 11 presents values of $(C_D/C_L - dC_D/dC_L)$ at the minimum comfortable approach speeds for carrier and airfield landings for 19 aircraft types. Drag effects were the predominant reason for limiting the approach speed in eight cases, and the data for these are shown in Table II, with $1/T_{h_1}$ determined by Eq 17. Unfortunately, these particular data are not at all convincing as regards the applicability of $1/T_{h_1}$ as a pertinent criterion for determining minimum VFR approach speeds. About all they do show is that, where direct comparisons are available, the carrier landing approach speed is less than the corresponding VFR approach speed. This lack of correlation with $1/T_{h_1}$ may be due to differences between the test airplanes as regards throttle force–displacement or engine response characteristics, both of which would affect the pilot's work load and rating (e.g., Ref. 12) for a given value of $1/T_{h_1}$. If in fact such differences exist, although concrete evidence is lacking, the maximum negative value of $1/T_{h_1}$ in Table II might be indicative of a criterion value for otherwise "good" control dynamics.

Fortunately this question does not arise in the data of Ref. 12, which reports results of approach and landing flight tests in a given airplane using an automatic throttle to change the variation with speed of the total X force (thrust minus drag). The primary data related to establishing a maximum acceptable negative value of $1/T_{h_1}$ are in a plot of mean pilot rating versus the inverse of the time to double amplitude of the speed instability. The inverse time constant of the speed instability is noted in Ref. 12 as

$$\frac{1}{\tau} = -\frac{0.693}{T_2} = \frac{1}{m}\left(\frac{\partial D}{\partial u} - \frac{\partial T}{\partial u}\right) \qquad (19)$$

which is approximately $1/T_{h_1}$ (Eq 18).* The data (Fig. 10 of Ref. 12) stratify into three distinct regions as a function of $1/T_{h_1}$. For $1/T_{h_1}$ between zero and about -0.045, mean ratings lie in the band given by 4.0 ± 0.3; for $1/T_{h_1}$ between about -0.045 and -0.15, mean ratings are distributed about 4.8 ± 0.4; for $1/T_{h_1}$ less than -0.15, ratings increase linearly to about 7.0 at $1/T_{h_1} \doteq -0.35$. Considering that the first jump

*The relations in Eq 16–18 are usually very good approximations for $1/T_{h_1}$, which is determined exactly by factorization of the h/δ_e transfer function numerator.

in rating is indicative of the $1/T_{h_1}$ effect sought,* these data indicate a criterion value of about -0.045, not too much different than the maximum negative value (-0.0398) of Table II.

Reference 13, a fixed-base simulator study of supersonic transport longitudinal handling qualities for the approach and landing task, indirectly furnishes additional information on acceptable values of $1/T_{h_1}$ for VFR situations. Pilot ratings were obtained for IFR approaches with two simulated values of the speed–thrust-required stability parameter parameter $d(T_r/W)/dV$, one being zero and the second -0.0012 per knot. $1/T_{h_1}$ is directly related to this parameter, i.e.,

$$\frac{1}{T_{h_1}} \doteq g \frac{dV}{du} \frac{d(T_r/W)}{dV} \tag{20}$$

where V is in knots and u is in feet per second. The corresponding values of $1/T_{h_1}$ are zero and -0.023 sec^{-1}. The change from neutral to unstable speed–thrust characteristics adversely affected the pilot ratings by approximately one rating point on the Cooper scale; and the pilots' comments indicated that a small but distinct task was added to the normal heavy work load in the IFR approach. For $1/T_{h_1} = -0.023$ sec^{-1} and positive static longitudinal stability, pilot ratings were generally 4.0 or slightly worse, indicating this value of $1/T_{h_1}$, although unsatisfactory for normal IFR operation, is not unacceptable. In the second phase of these studies, flare and touchdown evaluations were made in simulated VFR conditions. Numerical pilot ratings were not obtained. However, pilots commented that the effects of test variables (static longitudinal stability and speed–thrust stability) were minimized in the VFR task. Reference 4, reporting portions of the same investigation, also states that a review of flight experience indicated that in visual landing approaches the

*Retaining $1/T_{h_1}$ as a possible correlating parameter is based on the fact that it seems the only logical alternative to the reversal parameter, considered as most appropriate for carrier approaches. Since Table II clearly shows important differences between carrier and airfield approach speeds, it follows that different criteria <u>are</u> involved.

effect of speed–thrust instability is considerably less disturbing than in an IFR situation. It would appear from these results that values of $1/T_{h_1}$ more negative than -0.023 sec^{-1} would be acceptable in VFR approaches.

Although the flight and simulator data in Refs. 11–13 do not lead conclusively to a single maximum negative level of $1/T_{h_1}$ which can be used as a criterion for predicting VFR approach speeds, the range from -0.040 to -0.045 sec^{-1} may be a reasonable bound.

C. PREDICTED SPEEDS FOR THE OGEE WING F5D-1

The variations of $1/T_{h_1}$ with approach speed for three Ogee Wing F5D-1 configurations (basic, low drag, and high drag) are shown in Fig. 8. In each case the effect of c.g. location is indicated. It is assumed that landing gear and dive brake positions modify only the drag coefficient, and c.g. position changes only M_α. Values of $1/T_{h_1}$ are computed from dimensional stability and control derivatives using the relationship

$$\frac{1}{T_{h_1}} = \frac{X_{\delta_e} Z_u M_\alpha - Z_{\delta_e} X_u M_\alpha + M_{\delta_e}\left[Z_\alpha X_u - Z_u(X_\alpha - g)\right]}{X_{\delta_e} Z_u M_q - Z_{\delta_e}(X_u M_q - M_\alpha) - M_{\delta_e} Z_\alpha} \tag{21}$$

which is the ratio of the last two coefficients in the numerator of the altitude-to-elevator transfer function,* with $M_u = M_{\dot\alpha} = 0$ (Ref. 6). For the nominal c.g. location at 0.15 $\bar{c}_{F5D}$, the predicted approach speed ranges for VFR flight, based on a $1/T_{h_1}$ variation from -0.040 to -0.045, are:

CONFIGURATION	GEAR	DIVE BRAKES	U_o (knots)
Basic.....	Down	Closed	123–126
Low drag.....	Up	Closed	126–129
High drag.....	Down	Open	120–122

*For $\gamma_o = 0$. If the equations of motion are written to include nonzero flight path terms, the perturbation in vertical altitude is determined from $\dot{h} = -w\cos\gamma_o + u\sin\gamma_o + (U_o\cos\gamma_o)\theta$. However, the displacement normal to the flight path is found from $\dot{h} = U_o\theta - w$ and is the "effective" altitude controlled by the pilot. Use of this latter kinematic relationship rather than the former is equivalent to setting γ_o equal to zero.

Compared with the reversal parameter approach speed predictions for carrier approach, these results indicate the following:

1. For the nominal c.g. location, the difference between the approach speeds for the low and high drag configurations is less (6 – 7 knots) than the corresponding increment for carrier approaches (10 knots).

2. The $1/T_{h_1}$ predicted approach speeds for the c.g. at 0.15 $\bar{c}_{F5D}$ are slightly greater than the reversal parameter speeds for the basic and high drag configurations, and bracket the reversal parameter speed for the low drag configuration.

3. Static longitudinal stability effects are smaller, with a five percent forward shift in the c.g. location increasing the predicted speeds by 2 knots compared to 5.5 knots when the reversal parameter criterion is used.

4. The low drag, forward c.g. configuration has the largest difference in approach speed predictions based on $1/T_{h_1}$ and reversal parameter criteria. With the c.g. at 0.12 $\bar{c}_{F5D}$, the VFR predicted speeds are 128 – 130 knots and the carrier approach speeds are 138 ± 8 knots based on reversal parameter values of zero and ±0.001.

SECTION V

CONCLUSIONS

Prediction of minimum comfortable approach speeds based on closed-loop pilot-vehicle considerations requires knowledge of the specific loop closures made by the pilot. For optically aided carrier landings, the information available to the pilot in a completely (or nearly full-time) head-up approach is restricted to pitch attitude errors and altitude deviations from the glide path. Assuming the former is controlled with the elevator and the latter controlled with throttle, a reversal phenomenon may occur with reduction in approach speed, and a simple analytical criterion can be used to establish a minimum speed. Available data suggest the applicability of this prediction technique to the Ogee Wing F5D-1.

For VFR landings, there is no experimental evidence to directly indicate what information is sensed and used by the pilot. However, two loop closures are perhaps applicable. The first involves pitch attitude and altitude control with the elevator, appropriate for a "tight" VFR approach. The second assumes control of pitch attitude and rate of sink with the elevator in a "loose" VFR situation where the pilot is primarily concerned with the point of touchdown rather than with maintaining accurate glide path control. For both techniques, an instability, primarily in airspeed, will occur if the aircraft is on the back side of the drag curve. This instability can be stabilized with an airspeed to throttle loop, but the amount of instability and the required stabilizing throttle activity will progressively increase with reduced approach speeds. The pilot's throttle workload is proportional to the closed-loop instability encountered and, in turn, proportional to the open-loop low frequency zero, $1/T_{h_1}$, in the altitude-to-elevator transfer function. This open-loop parameter appears to adequately represent the control difficulties encountered in VFR approaches, and limiting values can be used as a criterion to predict minimum comfortable approach speeds in such cases.

Airplane drag characteristics have a strong influence on the criteria for both types of approaches, and for the Ogee Wing F5D-1 the increase in predicted approach speeds from a high to a low drag configuration for VFR approaches is less than the corresponding change for carrier approaches. Changes in static longitudinal stability have a more pronounced effect on predicted minimum acceptable speeds for mirror-aided carrier approaches than for airfield VFR approaches.

The low drag, forward c.g. configuration of the Ogee Wing F5D-1 offers the most promise for revealing differences in predicted approach speeds based on the two criteria.

REFERENCES

1. White, M. D., B. A. Schlaff, and F. J. Drinkwater, III, A Comparison of Flight-Measured Carrier-Approach Speeds with Values Predicted by Several Different Criteria for 41 Fighter-Type Airplane Configurations, NACA RM A57L11, May 1958.

2. Drinkwater, F. J., III, G. E. Cooper, and M. D. White, An Evaluation of the Factors Which Influence the Selection of Landing Approach Speeds, AGARD Rept. 230, 1958.

3. Drinkwater, F. J., III, and G. E. Cooper, A Flight Evaluation of the Factors Which Influence the Selection of Landing Approach Speeds, NASA Memo 10-6-58A, Dec. 1958.

4. Bray, R. S., "Piloted Simulator Studies Pertaining to the Low-Speed Longitudinal Handling Qualities of a Supersonic Transport Airplane," AIAA Simulation for Aerospace Flight Conference, A Volume of Technical Papers Presented Aug. 26-28, 1963, Columbus, Ohio, AIAA, New York, 1963, pp. 35-43.

5. Ashkenas, I. L., and D. T. McRuer, "A Theory of Handling Qualities Derived from Pilot-Vehicle System Considerations," Aerospace Eng., Vol. 21, No. 2, Feb. 1962, pp. 60, 61, 83-102.

6. Cromwell, C. H., and I. L. Ashkenas, A Systems Analysis of Longitudinal Piloted Control in Carrier Approach, Systems Technology, Inc., TR-124-1, June 1962.

7. Ashkenas, I. L., and T. S. Durand, "Simulator and Analytical Studies of Fundamental Longitudinal Control Problems in Carrier Approach," AIAA Simulation for Aerospace Flight Conference, A Volume of Technical Papers Presented Aug. 26-28, 1963, Columbus, Ohio, AIAA, New York, 1963, pp. 16-34.

8. Powers, B. G., and N. W. Matheny, Flight Evaluation of Three Techniques of Demonstrating the Minimum Flying Speed of a Delta-Wing Airplane, NASA TN D-2337, July 1964.

9. Radoll, R. W., Aerodynamic Data for Model F5D-1 Operational Flight Trainer, Douglas Aircraft Co., Inc., Rept. ES-26257, Apr. 1956.

10. Durand, T. S., and G. Teper, An Analysis of Terminal Flight Path Control in Carrier Landings, Systems Technology, Inc., TR-137-1, Aug. 1964.

11. Lean, D., and R. Eaton, The Influence of Drag Characteristics on the Choice of Landing Approach Speeds, AGARD Rept. 122, 1957.

12. Staples, K. J., Flight Measurements of the Influence of Speed Stability on the Landing Approach, AGARD Rept. 420, 1963.

13. Bray, R. S., A Piloted Simulator Study of Longitudinal Handling Qualities of Supersonic Transports in the Landing Maneuver, NASA TN D-2251, Apr. 1964.

14. Ashkenas, I. L., and D. T. McRuer, Approximate Airframe Transfer Functions and Application to Single Sensor Control Systems, WADC-TR-58-82, June 1958.

15. McRuer, D. T., I. L. Ashkenas, and H. R. Pass, Analysis of Multiloop Vehicular Control Systems, ASD-TDR-62-1014, Mar. 1964.

APPENDIX A

STABILITY DERIVATIVES AND TRANSFER FUNCTIONS

Longitudinal nondimensional stability and control derivatives for six trimmed lift coefficients with the center of gravity at the nominal 0.15 $\bar{c}_{F5D}$ location are presented in Table A-I. The pitch damping derivative, C_{m_q}, was obtained from Ref. 9; the other derivatives were computed from the full scale wind tunnel data of Fig. 2. Geometric and inertial properties used in calculating the dimensional derivatives in Table A-I are:

$$S = 661 \text{ ft}^2$$
$$c = 22.6 \text{ ft}$$
$$m = 612 \text{ slugs}$$
$$W = 19{,}700 \text{ lb}$$
$$I_{yy} = 70{,}600 \text{ slug-ft}^2$$

Atmospheric density corresponded to sea level standard conditions. The steady-state airspeeds are for power-on equilibrium flight at the listed trimmed lift coefficients with a flight path angle, γ_o, of -4 deg. The engine net thrust per unit throttle deflection, T_{δ_T}, of the F5D-1 was not available; therefore numerical values of throttle dimensional derivatives and gains of the throttle transfer function numerators are normalized with respect to T_{δ_T}.

Table A-II contains vehicle numerical transfer function data for both elevator and throttle inputs. Transfer functions are based on the following longitudinal linearized constant-coefficient equations of motion for stability axes:

$$\begin{aligned}
(s - X_u)u + (-X_w)w + (g \cos \gamma_o)\theta &= X_{\delta_e}\delta_e + X_{\delta_T}\delta_T \\
(-Z_u)u + (s - Z_w)w + (-U_o s + g \sin \gamma_o)\theta &= Z_{\delta_e}\delta_e + Z_{\delta_T}\delta_T \qquad \text{(A-1)} \\
(-M_u)u + (-M_{\dot{w}}s - M_w)w + (s^2 - M_q s)\theta &= M_{\delta_e}\delta_e + M_{\delta_T}\delta_T
\end{aligned}$$

where s is the Laplace transform variable. The auxiliary equation for airplane displacement normal to the flight path, h, is

$$h = \frac{1}{s}(U_o\theta - w) \tag{A-2}$$

All transfer functions, including those for the auxiliary variable h, have the same denominator, Δ. Thus,

$$\frac{\theta(s)}{\delta_e(s)} = \frac{N_{\theta\delta_e}}{\Delta} \quad ; \quad \frac{u(s)}{\delta_T(s)} = \frac{N_{u\delta_T}}{\Delta} \quad ; \quad \frac{h(s)}{\delta_e(s)} = \frac{N_{h\delta_e}}{\Delta} \quad ; \quad \text{etc.}$$

where

$$\Delta = \begin{vmatrix} (s - X_u) & -X_w & g\cos\gamma_o \\ -Z_u & (s - Z_w) & (-U_o s + g\sin\gamma_o) \\ -M_u & (-M_{\dot{w}}s - M_w) & (s^2 - M_q s) \end{vmatrix} \tag{A-3}$$

$$N_{\theta\delta_e} = \begin{vmatrix} (s - X_u) & -X_w & X_{\delta_e} \\ -Z_u & (s - Z_w) & Z_{\delta_e} \\ -M_u & (-M_{\dot{w}}s - M_w) & M_{\delta_e} \end{vmatrix} \tag{A-4}$$

$$N_{u\delta_T} = \begin{vmatrix} X_{\delta_T} & -X_w & g\cos\gamma_o \\ Z_{\delta_T} & (s - Z_w) & (-U_o s + g\sin\gamma_o) \\ M_{\delta_T} & (-M_{\dot{w}}s - M_w) & (s^2 - M_q s) \end{vmatrix} \tag{A-5}$$

$$N_{h\delta_e} = \frac{U_o}{s} N_{\theta\delta_e} - \frac{1}{s} N_{w\delta_e} \tag{A-6}$$

$$N_{h_{\delta_e}} = \begin{vmatrix} (s - X_u) & -X_w & g \cos \gamma_o & X_{\delta_e} \\ -Z_u & (s - Z_w) & (-U_o s + g \sin \gamma_o) & Z_{\delta_e} \\ -M_u & (-\dot{M_w} s - M_w) & (s^2 - M_q s) & M_{\delta_e} \\ 0 & 1/s & -U_o/s & 0 \end{vmatrix} \quad \text{(A-7)}$$

Coupling numerators (Ref. 15) used in multiloop closures are also presented. They are similar to conventional transfer function numerators with two columns of the characteristic determinant replaced by appropriate control effectiveness terms. For example,

$$N_{\delta_e \delta_T}^{\theta \; u} = \begin{vmatrix} X_{\delta_T} & -X_w & X_{\delta_e} \\ Z_{\delta_T} & (s - Z_w) & Z_{\delta_e} \\ M_{\delta_T} & (-\dot{M_w} s - M_w) & M_{\delta_e} \end{vmatrix} \quad \text{(A-8)}$$

TABLE I

EFFECTS OF APPROACH SPEED ON $\theta,h \rightarrow \delta_e$ PARAMETERS FOR THE OGEE WING F5D-1

U_o (knots)	$1/T''_{h_1}$ (sec^{-1})	ω''_p (rad/sec)	ζ''_p	ω''_{sp} (rad/sec)	ζ''_{sp}	ω_c (rad/sec)	φ_m (deg)	$K_{\delta_{eh}}$ (rad/ft)
131	−0.0247	0.75	0.35	1.13	0.51	0.50	44	−0.00083
123	−0.0385	0.60	0.35	1.33	0.43	0.43	47	−0.00095
118.5	−0.0474	0.55	0.35	1.40	0.41	0.43	44	−0.00103
114.5	−0.0532	0.50	0.35	1.41	0.40	0.37	52	−0.00098

TABLE II

CHARACTERISTICS AT MINIMUM COMFORTABLE APPROACH SPEEDS (DATA FROM REF. 11)

AIR-CRAFT TYPE	CARRIER LANDING			AIRFIELD LANDING		
	APPROACH SPEED (knots)	$\left(\frac{C_D}{C_L} - \frac{dC_D}{dC_L}\right)$	$1/T_{h_1}$ (sec^{-1})	APPROACH SPEED (knots)	$\left(\frac{C_D}{C_L} - \frac{dC_D}{dC_L}\right)$	$1/T_{h_1}$ (sec^{-1})
A				120	0.030	0.0095
B				110	−0.011	−0.0038
C	101	−0.030	−0.0113	107	0.014	0.0050
D	85	−0.127	−0.0570	90	−0.091	−0.0385
E				160	−0.089	−0.0212
F				135	−0.141	−0.0398
G	128	−0.079	−0.0235			
I				118	0.046	0.0149

TABLE A-I

OGEE WING F5D-1 NONDIMENSIONAL AND DIMENSIONAL STABILITY DERIVATIVES

U_o (knots)	147	131	123	118.5	114.5	109
$C_{L_{trim}}$	0.40	0.50	0.56	0.60	0.64	0.70
α_{trim} (deg)	9.5	11.5	12.7	13.5	14.4	15.7
$\delta_{e_{trim}}$ (deg)	−4.1	−4.4	−4.6	−4.7	−4.9	−5.3
C_{L_α} (1/rad)	3.10	3.01	2.92	2.87	2.85	2.81
$C_{L_{\delta_e}}$ (1/rad)	0.756	0.768	0.760	0.756	0.751	0.745
C_D	0.086	0.116	0.136	0.153	0.174	0.203
C_{D_α} (1/rad)	0.803	1.00	1.15	1.26	1.38	1.55
$C_{D_{\delta_e}}$ (1/rad)	0.103	0.137	0.148	0.155	0.166	0.183
C_{m_α} (1/rad)	−0.0800	−0.0344	−0.0740	−0.0975	−0.116	−0.138
C_{m_q} (1/rad)	−1.1	−1.1	−1.1	−1.1	−1.1	−1.1
$C_{m_{\delta_e}}$ (1/rad)	−0.321	−0.332	−0.330	−0.326	−0.317	−0.309
X_u (1/sec)	−0.0548	−0.0658	−0.0727	−0.0786	−0.0863	−0.0959
Z_u (1/sec)	−0.255	−0.284	−0.299	−0.308	−0.317	−0.331
M_u (1/sec-ft)	0	0	0	0	0	0
X_w (1/sec)	−0.128	−0.142	−0.158	−0.170	−0.182	−0.200
Z_w (1/sec)	−1.01	−0.887	−0.816	−0.776	−0.748	−0.712
M_w (1/sec-ft)	−0.00499	−0.00191	−0.00387	−0.00491	−0.00563	−0.00637
$M_{\dot{\alpha}}$ (1/sec^2)	−1.24	−0.423	−0.805	−0.981	−1.09	−1.17
$M_{\dot{w}}$ (1/ft)	0	0	0	0	0	0
M_q (1/sec)	−0.776	−0.691	−0.650	−0.625	−0.604	−0.575
X_{δ_e} (ft/sec^2)	−8.14	−8.62	−8.22	−7.96	−7.94	−7.96
Z_{δ_e} (ft/sec^2)	−59.7	−48.2	−42.2	−38.8	−35.9	−32.4
M_{δ_e} (1/sec^2)	−4.97	−4.08	−3.59	−3.28	−2.97	−2.63
$X_{\delta_T}/T_{\delta_T}$ (ft/sec^2-lb)	0.00161	0.00160	0.00159	0.00159	0.00158	0.00157
$Z_{\delta_T}/T_{\delta_T}$ (ft/sec^2-lb)	−0.000271	−0.000326	−0.000359	−0.000382	−0.000405	−0.000442
$M_{\delta_T}/T_{\delta_T}$ (1/sec^2-lb)	0	0	0	0	0	0

TABLE A-II

OGEE WING F5D-1 LONGITUDINAL TRANSFER FUNCTIONS

U_o (knots)	147	131	123	118.5	114.5	109
$C_{L_{trim}}$	0.40	0.50	0.56	0.60	0.64	0.70
$\Delta = \left[s^2 + 2\zeta_p\omega_p s + \omega_p^2\right]\left[s^2 + 2\zeta_{sp}\omega_{sp}s + \omega_{sp}^2\right]$						
ζ_p	0.103	0.0634	0.0714	0.0824	0.0945	0.104
ω_p (rad/sec)	0.143	0.130	0.169	0.185	0.197	0.212
ζ_{sp}	0.639	0.792	0.657	0.603	0.571	0.540
ω_{sp} (rad/sec)	1.42	1.03	1.15	1.20	1.23	1.24
$N_{\theta\delta_e} = A_{\theta\delta_e}(s + 1/T_{\theta_1})(s + 1/T_{\theta_2})$						
$A_{\theta\delta_e}$ ($1/sec^2$)	-4.97	-4.08	-3.59	-3.28	-2.97	-2.63
$1/T_{\theta_1}$ (1/sec)	0.0220	0.0195	0.0139	0.0100	0.00744	0.00119
$1/T_{\theta_2}$ (1/sec)	0.988	0.911	0.830	0.787	0.759	0.728
$N_{u\delta_e} = A_{u\delta_e}(s + 1/T_{u_1})(s + 1/T_{u_2})(s + 1/T_{u_3})$						
$A_{u\delta_e}$ (ft/sec^2-rad)	-8.14	-8.62	-8.22	-7.96	-7.94	-7.96
$1/T_{u_1}$ (1/sec)	0.498	0.447	0.397	0.367	0.344	0.316
$1/T_{u_2}$ (1/sec)	6.34	5.62	5.39	5.24	5.01	4.74
$1/T_{u_3}$ (1/sec)	-5.99	-5.28	-5.13	-5.03	-4.83	-4.59

Table A-II (Continued)

U_o (knots)	147	131	123	118.5	114.5	109
$C_{L_{trim}}$	0.40	0.50	0.56	0.60	0.64	0.70
$N_{u\delta_T} = A_{u\delta_T}(s + 1/T_{u_T})\left[s^2 + 2\zeta_u\omega_u s + \omega_u^2\right]$						
$A_{u\delta_T}/T_{\delta_T}$ (ft/sec^2-lb)	0.00161	0.00160	0.00159	0.00159	0.00158	0.00157
$1/T_{u_T}$ (1/sec)	−0.00767	−0.00768	−0.0140	−0.0177	−0.0211	−0.0261
ζ_u	0.635	0.781	0.645	0.593	0.562	0.533
ω_u (rad/sec)	1.43	1.03	1.18	1.23	1.26	1.28
$sN_{h\delta_e} = A_{h\delta_e}(s + 1/T_{h_1})(s + 1/T_{h_2})(s + 1/T_{h_3})$						
$A_{h\delta_e}$ (ft/sec^2-rad)	59.7	48.2	42.2	38.8	35.9	32.4
$1/T_{h_1}$ (1/sec)	−0.0123	−0.0276	−0.0455	−0.0585	−0.0699	−0.0903
$1/T_{h_2}$ (1/sec)	−4.05	−3.67	−3.35	−3.15	−2.97	−2.76
$1/T_{h_3}$ (1/sec)	4.85	4.40	4.05	3.84	3.65	3.42
$sN_{h\delta_T} = A_{h\delta_T}(s + 1/T_{h_T})\left[s^2 + 2\zeta_h\omega_h s + \omega_h^2\right]$						
$A_{h\delta_T}/T_{\delta_T}$ (ft/sec^2-lb)	0.000271	0.000326	0.000359	0.000382	0.000405	0.000442
$1/T_{h_T}$ (1/sec)	1.57	1.46	1.40	1.36	1.33	1.27
ζ_h	0.350	0.532	0.363	0.316	0.290	0.266
ω_h (rad/sec)	1.10	0.650	0.897	0.990	1.04	1.08

Table A-II (Concluded)

U_o (knots)	147	131	123	118.5	114.5	109
$C_{L_{trim}}$	0.40	0.50	0.56	0.60	0.64	0.70
$N^{\theta\ u}_{\delta_e \delta_T} = A_{\theta u}(s + 1/T_{\theta u})$						
$A_{\theta u}/T_{\delta_T}$ (ft/sec^4-lb)	−0.00800	−0.00653	−0.00573	−0.00521	−0.00470	−0.00414
$1/T_{\theta u}$ (1/sec)	0.975	0.893	0.804	0.756	0.723	0.684
$sN^{h\ u}_{\delta_e \delta_T} = A_{hu}(s + 1/T_{hu_1})(s + 1/T_{hu_2})$						
A_{hu}/T_{δ_T} (ft^2/sec^4-lb-rad)..	0.0984	0.0800	0.0704	0.0646	0.0601	0.0545
$1/T_{hu_1}$ (1/sec)	4.87	4.42	4.09	3.88	3.69	3.48
$1/T_{hu_2}$ (1/sec)	−4.09	−3.73	−3.44	−3.25	−3.09	−2.90
$sN^{\theta\ h}_{\delta_e \delta_T} = A_{\theta h}(s + 1/T_{\theta h})$						
$A_{\theta h}/T_{\delta_T}$ (ft/sec^4-lb)	−0.00135	−0.00133	−0.00129	−0.00126	−0.00120	−0.00116
$1/T_{\theta h}$ (1/sec)	1.57	1.46	1.40	1.36	1.33	1.27

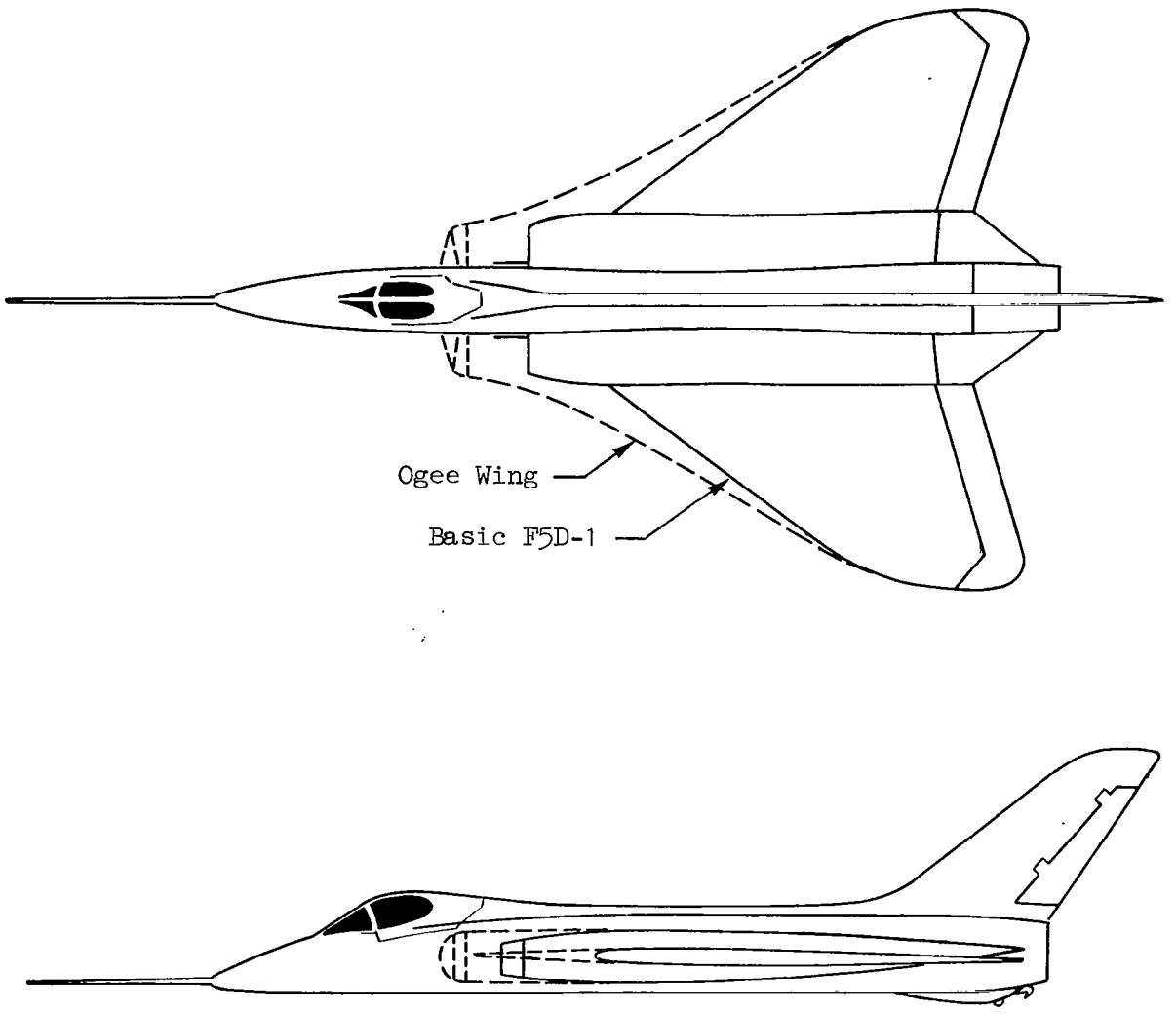

Figure 1. Drawing of Basic and Modified F5D-1 Airplane

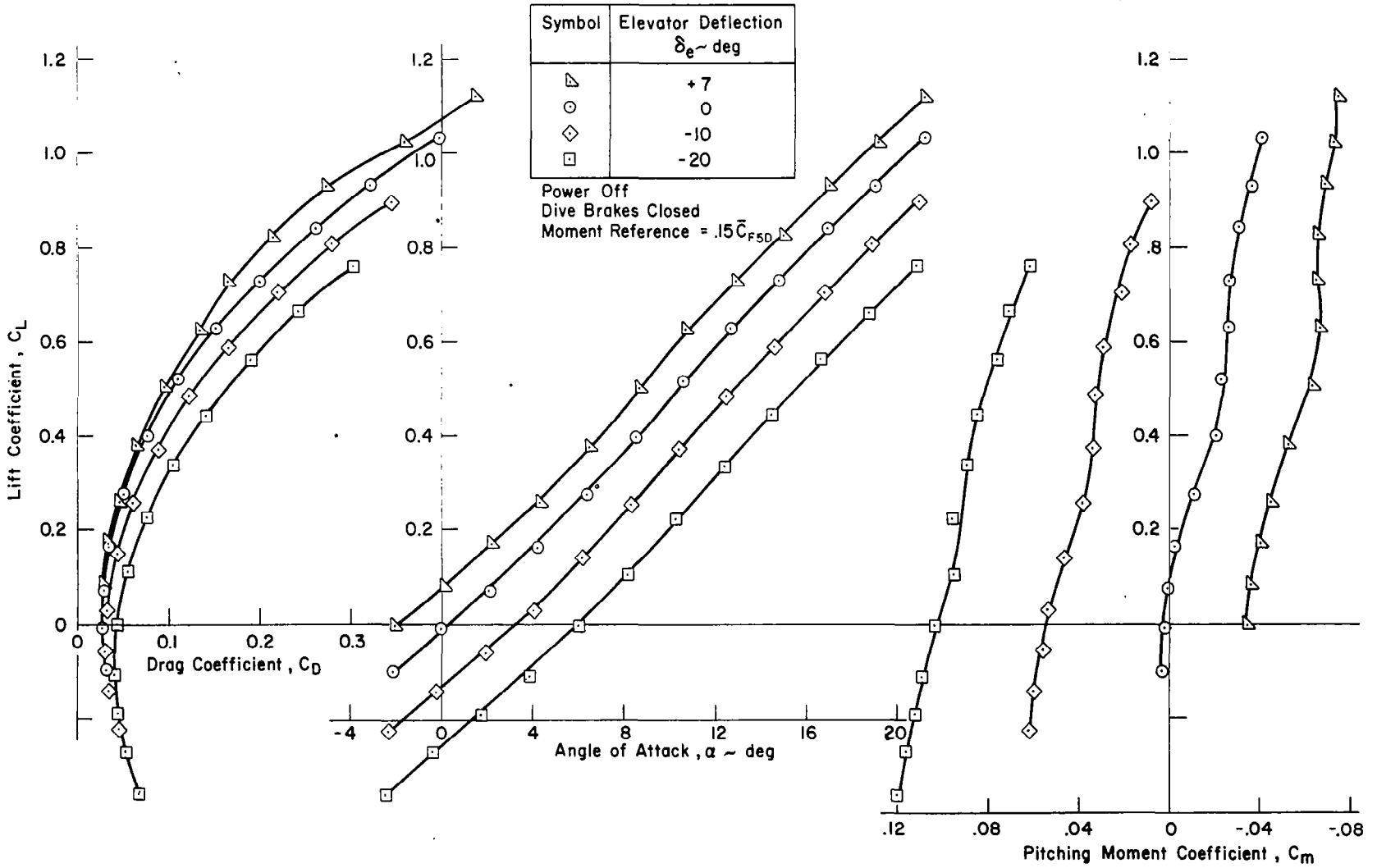

Figure 2. Basic Longitudinal Wind Tunnel Data

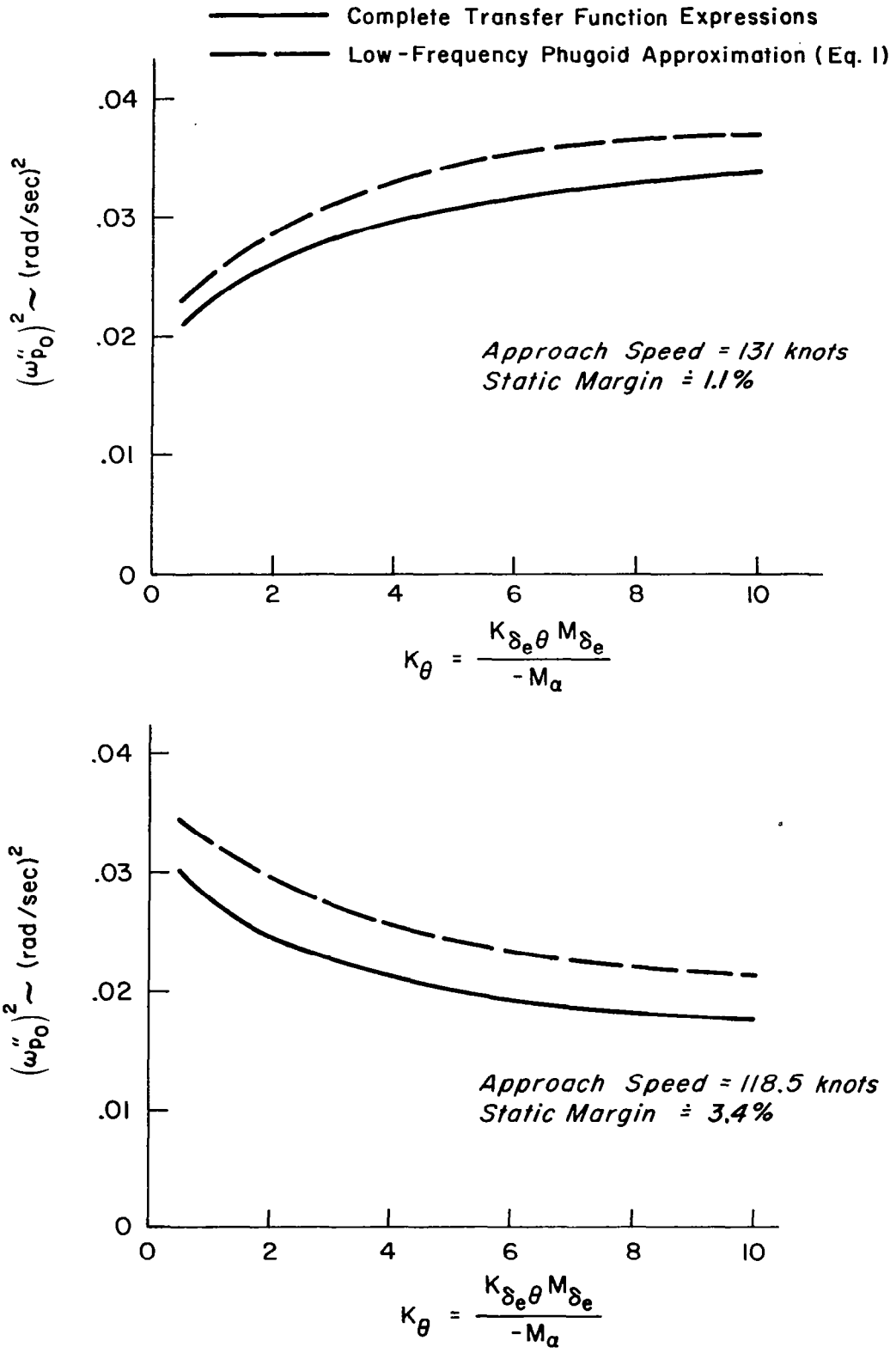

Figure 3. Evaluation of Phugoid Approximation in Reversal Parameter Derivation

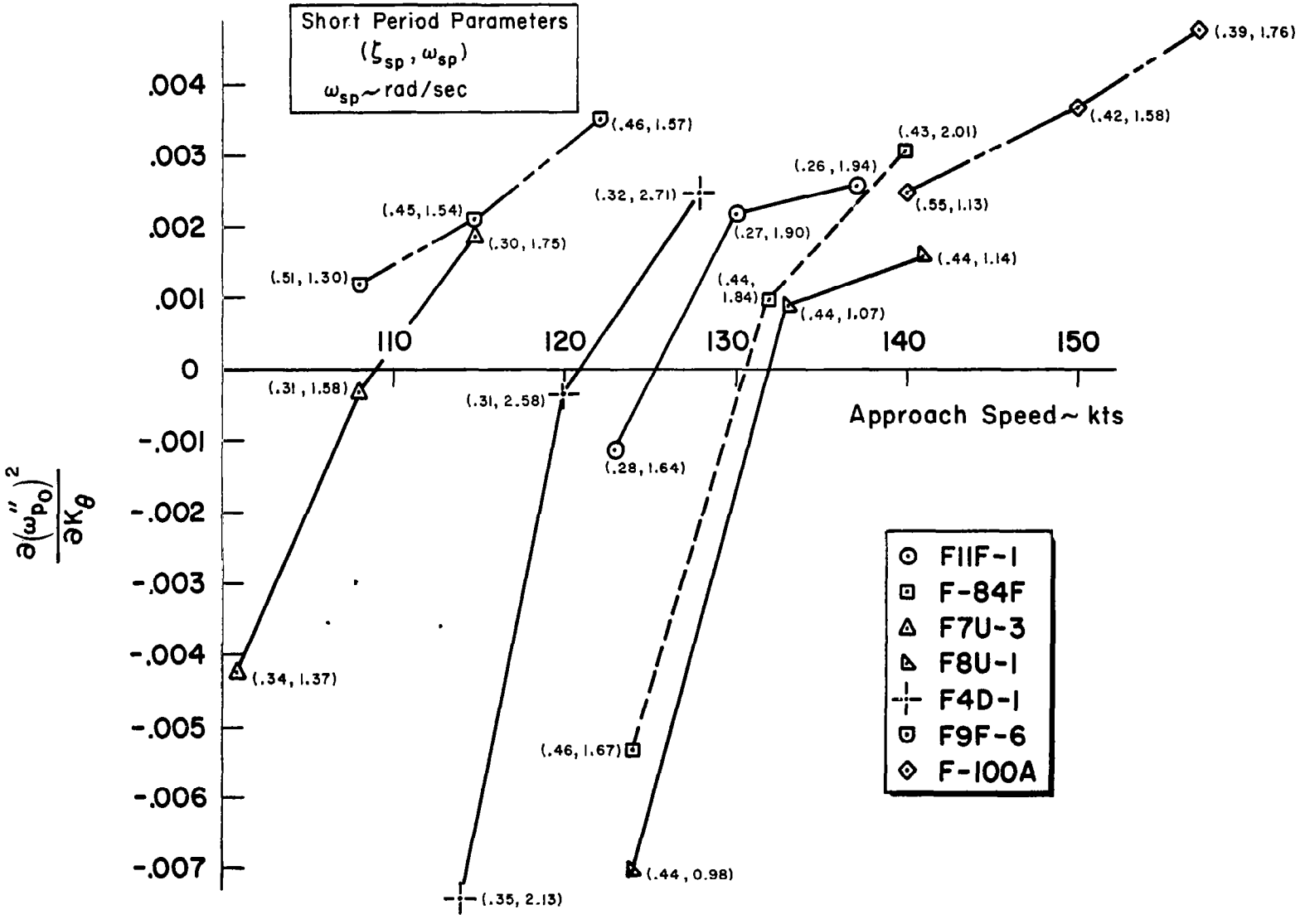

Figure 4. Short-Period Characteristics of Aircraft at Low Speeds
(Data from Ref. 6)

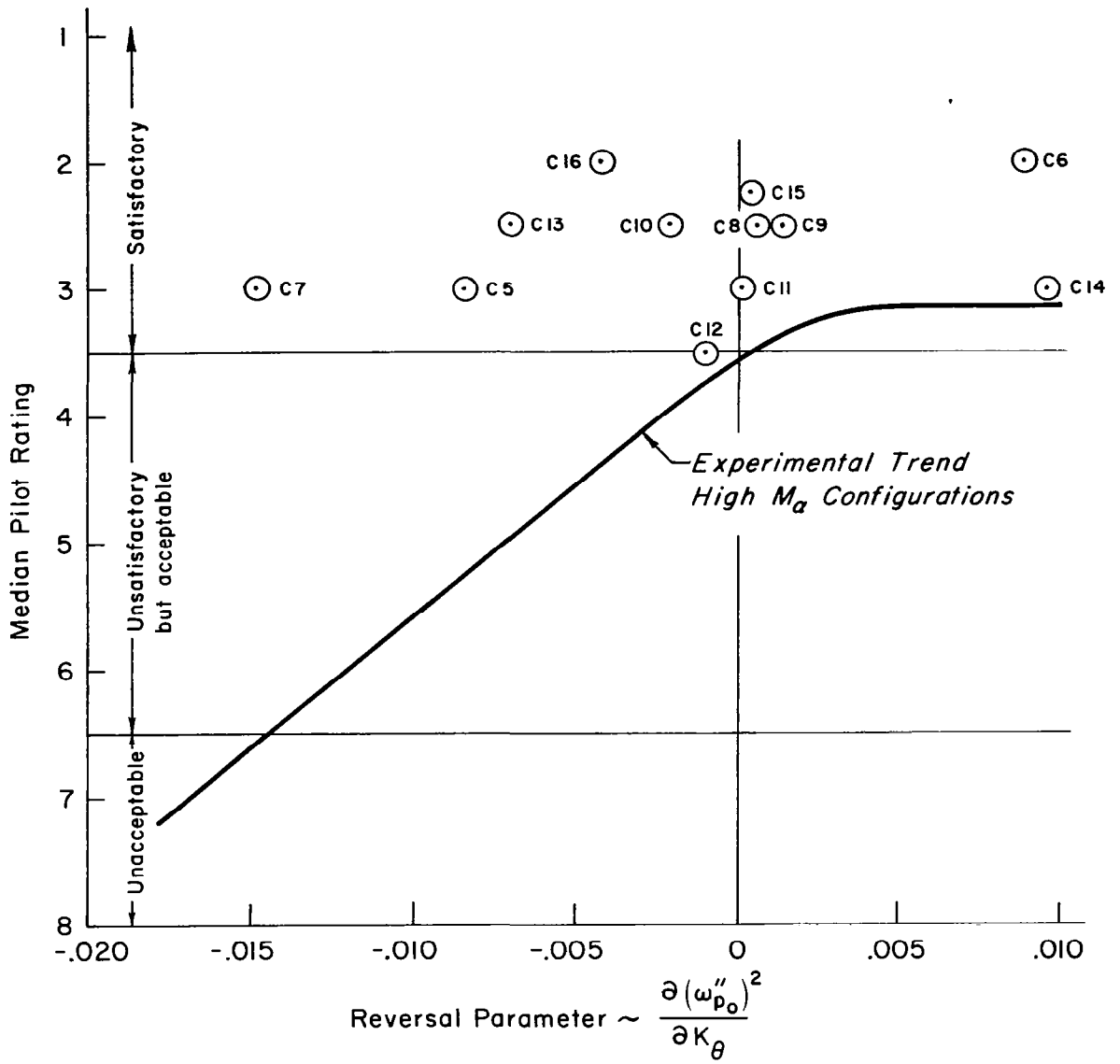

Figure 5. Pilot Rating Versus Reversal Parameter for Configurations with Low M_α; Simulator Results from Ref. 7

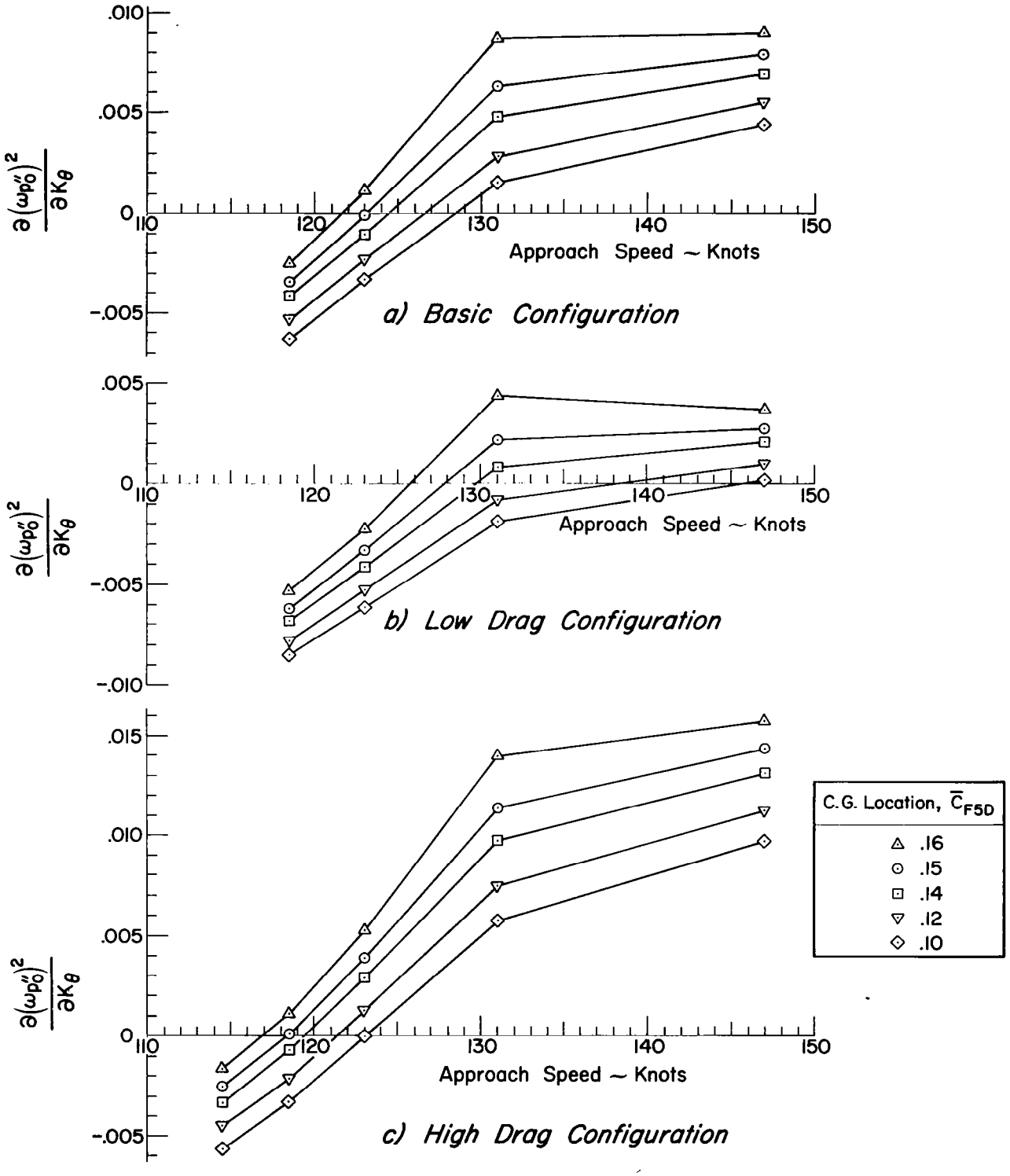

Figure 6. Reversal Parameter Versus Approach Speed

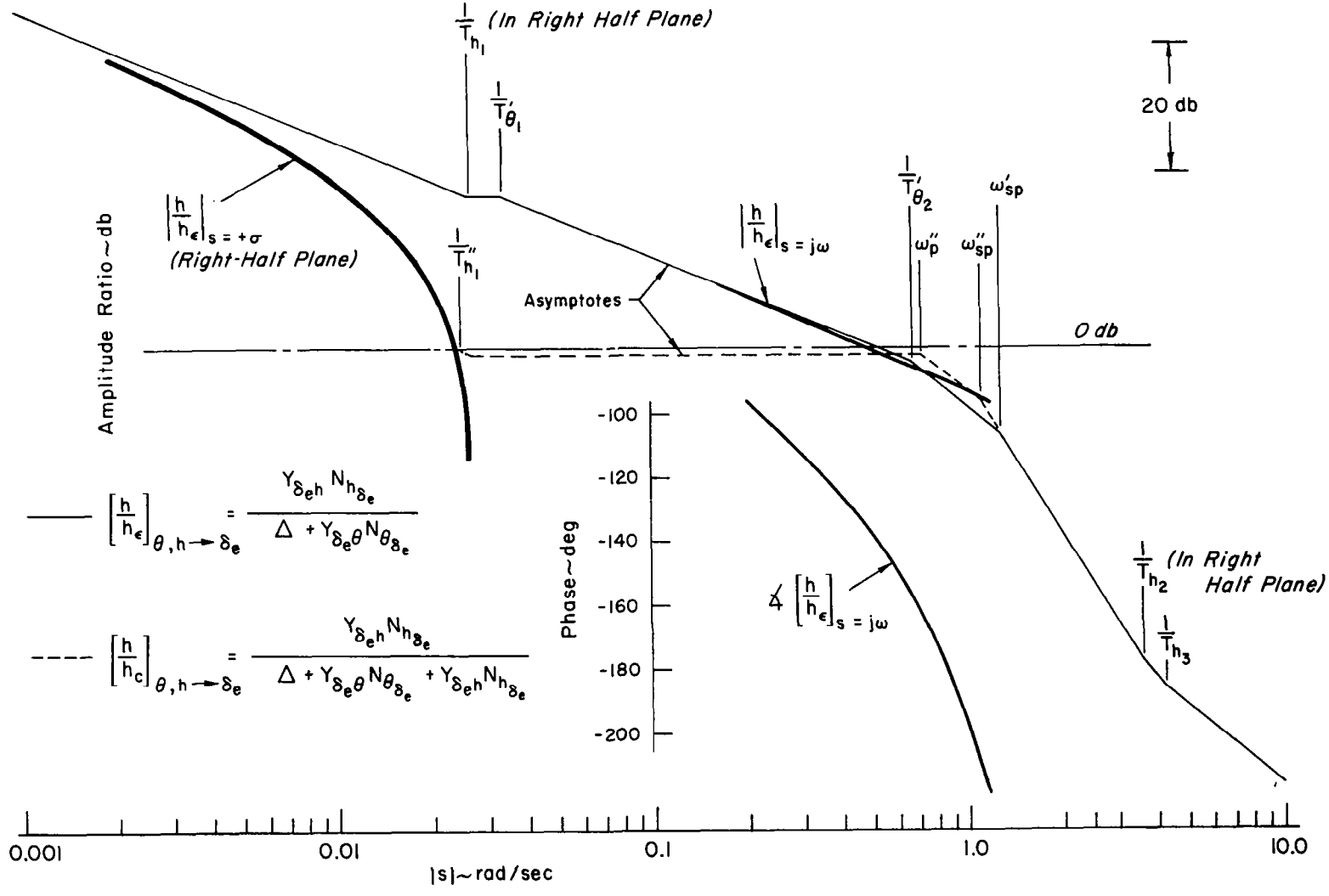

Figure 7. $\theta,h \rightarrow \delta_e$ Characteristics, Approach Speed = 131 Knots

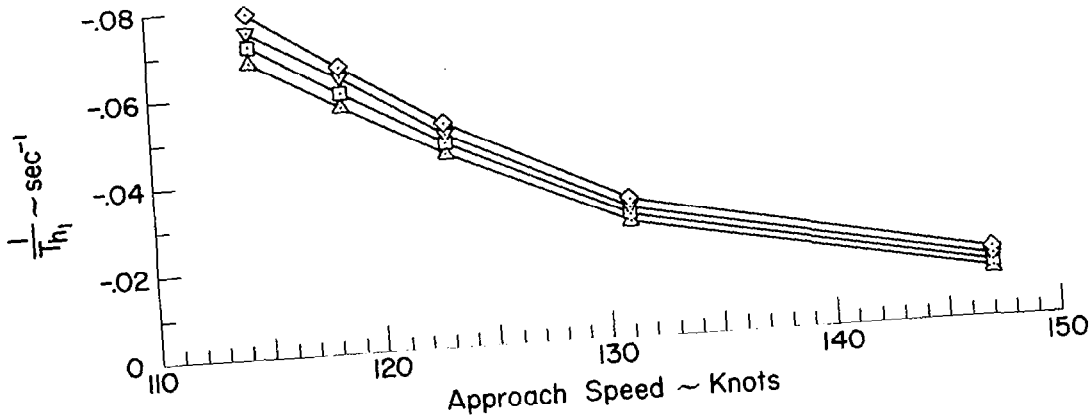

a) Basic Configuration

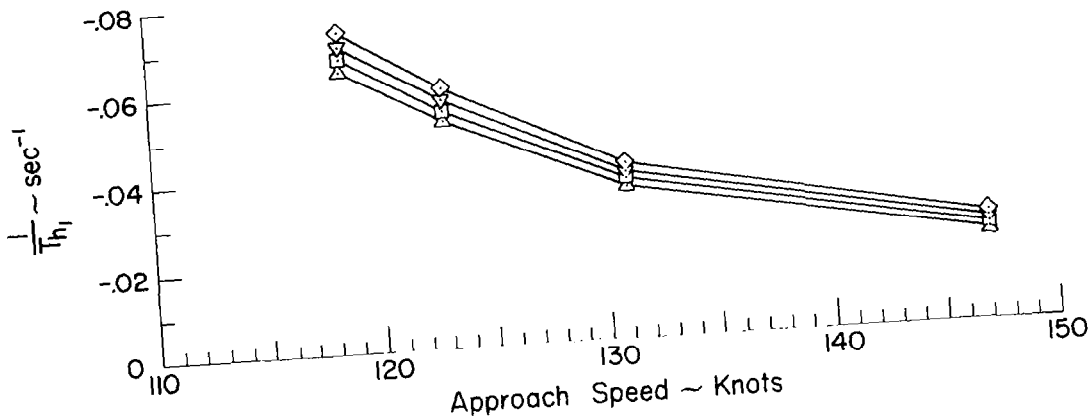

b) Low Drag Configuration

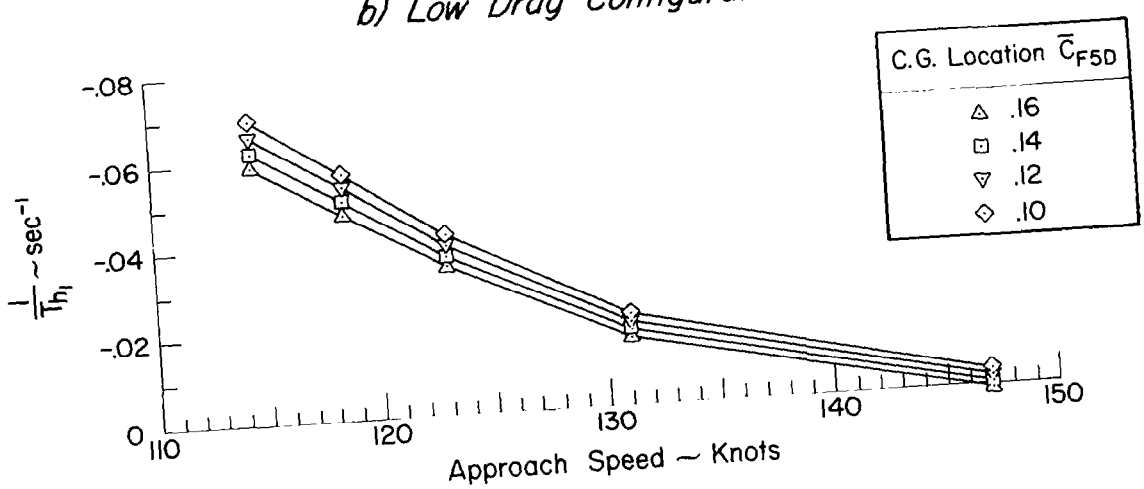

c) High Drag Configuration

Figure 8. $1/T_{h_1}$ Versus Approach Speed

NASA-Langley, 1966 CR-579

"The aeronautical and space activities of the United States shall be conducted so as to contribute . . . to the expansion of human knowledge of phenomena in the atmosphere and space. The Administration shall provide for the widest practicable and appropriate dissemination of information concerning its activities and the results thereof."

—NATIONAL AERONAUTICS AND SPACE ACT OF 1958

NASA SCIENTIFIC AND TECHNICAL PUBLICATIONS

TECHNICAL REPORTS: Scientific and technical information considered important, complete, and a lasting contribution to existing knowledge.

TECHNICAL NOTES: Information less broad in scope but nevertheless of importance as a contribution to existing knowledge.

TECHNICAL MEMORANDUMS: Information receiving limited distribution because of preliminary data, security classification, or other reasons.

CONTRACTOR REPORTS: Technical information generated in connection with a NASA contract or grant and released under NASA auspices.

TECHNICAL TRANSLATIONS: Information published in a foreign language considered to merit NASA distribution in English.

TECHNICAL REPRINTS: Information derived from NASA activities and initially published in the form of journal articles.

SPECIAL PUBLICATIONS: Information derived from or of value to NASA activities but not necessarily reporting the results of individual NASA-programmed scientific efforts. Publications include conference proceedings, monographs, data compilations, handbooks, sourcebooks, and special bibliographies.

Details on the availability of these publications may be obtained from:

SCIENTIFIC AND TECHNICAL INFORMATION DIVISION

NATIONAL AERONAUTICS AND SPACE ADMINISTRATION

Washington, D.C. 20546